The challenges of determining metal–protein affinities

Article *in* Natural Product Reports · April 2010

DOI: 10.1039/b906690j · Source: PubMed

2 authors:

Zhiguang Xiao
The Florey Institute of Neuroscience and Mental Health
77 PUBLICATIONS **2,232** CITATIONS
SEE PROFILE

Anthony G Wedd
University of Melbourne
294 PUBLICATIONS **7,083** CITATIONS
SEE PROFILE

The challenges of determining metal–protein affinities†‡

Zhiguang Xiao* and Anthony G. Wedd

Received 5th January 2010
First published as an Advance Article on the web 9th April 2010
DOI: 10.1039/b906690j

Covering: up to the end of 2009

A key property of metallo-proteins and -enzymes is the affinity of metal ion M for protein ligand P as defined by the dissociation constant $K_D = [M][P]/[MP]$. Its accurate determination is essential for a quantitative understanding of metal selection and speciation. However, the surfaces of proteins are defined by the sidechains of amino acids and so abound in good metal ligands (*e.g.*, imidazole of histidine, thiol of cysteine, carboxylate of aspartic and glutamic acids, *etc.*). Consequently, adventitious binding of metal ions to protein surfaces is common with K_D values $\geq 10^{-6}$ M. On the other hand, transport proteins responsible for 'chaperoning' essential metals to their cellular destinations appear to bind the metal ions *selectively* ($K_D < 10^{-7}$ M), both for speciation and to minimise the toxic effects of 'free' metal ions. These ions are normally bound with still higher affinities at their ultimate destinations (the active sites of metallo-proteins and -enzymes). This review surveys possible approaches to estimation of these dissociation constants and pinpoints the various problems associated with each approach.

School of Chemistry and Bio21 Molecular Science and Biotechnology Institute, University of Melbourne, Parkville, Victoria, 3010, Australia. E-mail: z.xiao@unimelb.edu.au

† This paper is part of an *NPR* themed issue on Metals in cells, guest-edited by Emma Raven and Nigel Robinson.

‡ Electronic supplementary information (ESI) available: Additional information on determination of Cu^{I} binding stoichiometry and affinity for Atox (Hah1) protein. See DOI: 10.1039/b906690j

1 Introduction

At this moment in time, quantitative characterization of biomolecules requires their isolation or synthesis followed by *in vitro* definition of structure and reactivity. This process provides data for correlation with *in vivo* experiments to evolve a molecular understanding of biological activity.[1]

For metallo-proteins and -enzymes, a key property is the affinity of metal ion M for protein ligand P as defined by the dissociation constant K_D (eqn (1)):

$$MP \rightleftharpoons M + P \quad K_D = \frac{[M][P]}{[MP]} \tag{1}$$

Adventitious binding of metal ions to protein surfaces is common under *in vitro* conditions with K_D values $\geq 10^{-6}$ M. Consequently, metallo-proteins and -enzymes must bind metals specifically with

higher affinities ($K_D < 10^{-7}$ M). On the other hand, transport proteins responsible for 'chaperoning' metals to their cellular destinations (*i.e.*, metallo-proteins and -enzymes)[1–3] also bind the metal ions *selectively* ($K_D < 10^{-7}$ M), both for speciation and to minimise the toxic effects[4] of 'free' redox-active metal ions.

Reliable evaluation and comparison of metal-binding affinities is important for a quantitative understanding of metal selection and speciation. However, estimation of these metal-binding constants is problematical at the moment, as disparate values have been reported in the literature. A few important examples serve as illustrative of a wider problem:

(1) The prion protein can bind multiple Cu^{2+} ions in versatile sites of the so-called octa-repeat region. Estimated K_D values range from 10^{-5}–10^{-9} M with one estimate of 10^{-14} M.[5–9]

(2) Reported K_D values for the Cu^{I} metallochaperones Atx1, Atox1, CopZ and related protein domains differ by more than 10 orders of magnitude even though their structures and metal-binding sites essentially superimpose.[10–15]

(3) Reported K_D values for the binding of Co^{2+} to the N-terminal zinc-binding peptide of the HIV-1 nucleocapsid protein vary by 6 orders of magnitude (10^{-6}–10^{-12} M).[16]

While the variation in (1) above may partially reflect different affinities at different sites[9] (*cf.* metallothioneins[17]), the other systems cited bind a single metal ion only. The reported discrepancies highlight the fact that accurate estimates are subject to a number of pitfalls and complicating factors, all of which must be avoided or kept under control. These include: (a) lack of effective competition in equilibrium experiments; (b) lack of effective control of pH and its influence upon the affinities of ligand probes; (c) neglect of the metal affinities of pH buffers; (d) aerial oxidation of binding sites; (e) presence of ternary complexes in the equilibrium mixture and (f) incorrect interpretation and processing of the experimental data. This review will present various case studies which pinpoint these potential problems.

2 Metal buffers

A ligand may act as a metal buffer if it can bind and exchange the metal ion M rapidly.[18,19] The effective concentration range (expressed as pM = −log[M]) that can be buffered depends on three factors: (i) the affinity of the ligand for the metal ion; (ii) the ligand concentration employed; (iii) the stoichiometry of the metal complex. The affinity of a ligand L for M is conventionally expressed by chemists as the apparent association constant (or formation constant) K_A' for 1:1 complexes and $\beta_2' = K_{A1}'K_{A2}'$ for 1:2 complexes under the conditions of measurement (eqn (2) and (3)):

$$M + L' \rightleftharpoons ML \quad K_A' = \frac{[ML]}{[M][L']} \tag{2}$$

$$M + 2L' \rightleftharpoons ML_2 \quad \beta_2' = \frac{[ML_2]}{[M][L']^2} \tag{3}$$

Throughout this review, L′ refers to all forms of ligand L in solution which are not bound to M. This usually means different protonation states.

In biology, the affinity of a protein ligand P for metal M is more frequently expressed as the dissociation constant K_D as defined by eqn (1). All K_D values for proteins are apparent constants defined under specific conditions but the symbol ′ is omitted for simplicity. Note that eqn (1) and (2) are equivalent: $K_D = 1/K_A'$. Using the K_D formalism, $[M] = K_D[ML]/[L']$, *i.e.*, the 'free' metal concentration [M] buffered by the couple (L′, ML) is constant at a fixed ratio [ML]/[L′], regardless of total metal and ligand concentrations (but under the condition that $[ML] \gg K_D$). In the special case of 50% metal occupancy of the ligand site, [ML] = [L′] and [M] = K_D (pM = − logK_D). An example is Cu^{2+} buffered by the couple (Edta′, $[Cu^{II}Edta]^{2-}$) at pH 7.0 with Cu^{II}: Edta′ = 1:2 (see Scheme 1 for ligand structures; Fig. 1a(i)). Thus, for 1:1 metal complexes, it is possible to compare metal affinities directly from the K_D (or K_A^{-1}) values.

However, the situation is very different for a 1:2 complex (eqn (3)). At 50% metal occupancy, $[L'] = 2[ML_2]$ and the 'free' metal concentration $[M] = (4[ML_2]\beta_2')^{-1}$. Then [M] is inversely proportional to both the association constant β_2' and the metal complex concentration $[ML_2]$. The 'free' metal concentration buffered by the couple (L′, ML_2) decreases (pM increases) with increases in the *total* concentrations of both ligand and metal ion under the constraint of a fixed ratio of $[L]_{total}/[M]_{total}$. An

Zhiguang Xiao

Zhiguang Xiao is a Research Fellow in the Bio21 Molecular Science and Biotechnology Research Institute and School of Chemistry at the University of Melbourne, Australia.

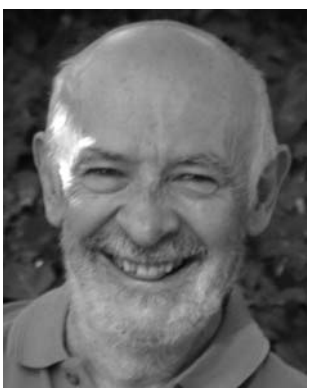

Anthony Wedd

Anthony Wedd is Professor of Chemistry in the Bio21 Molecular Science and Biotechnology Research Institute and School of Chemistry at the University of Melbourne, Australia.

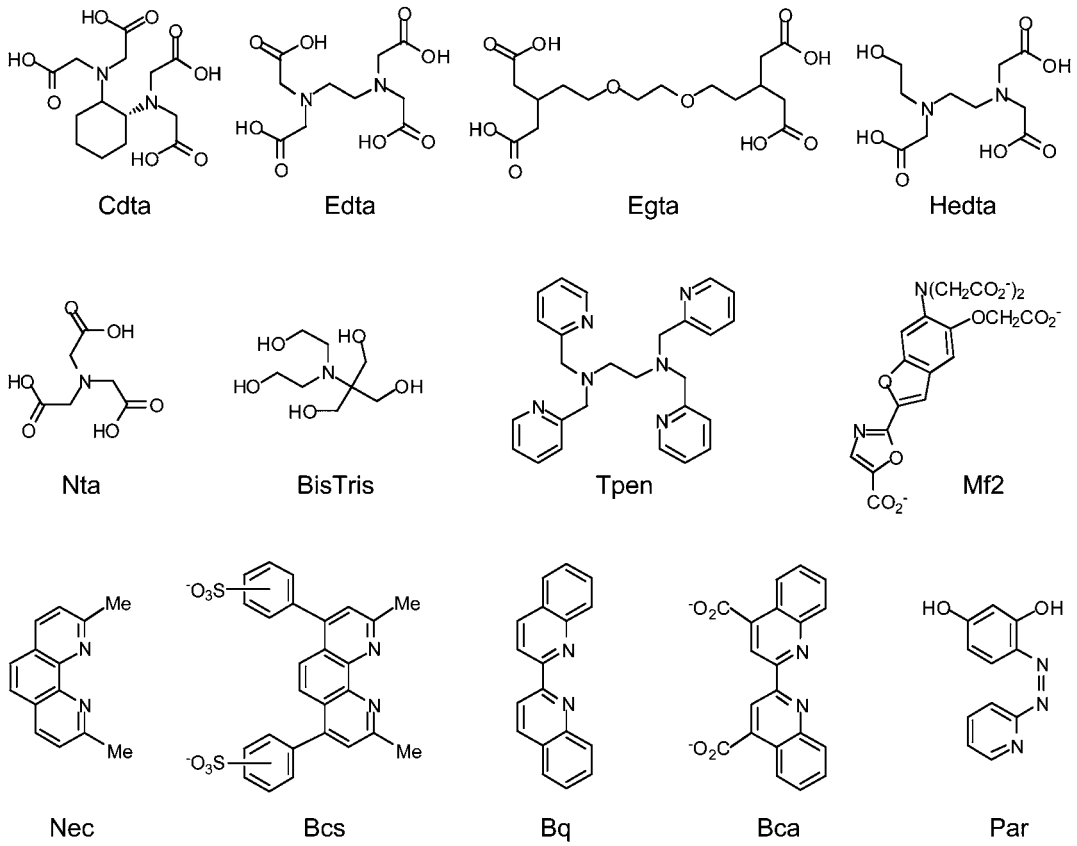

Scheme 1 Schematic representations of selected metal ligand structures.

example is shown in Fig. 1a(ii) for the case of Cu^{+} buffered by the couple (Bcs′, $[Cu^{I}(Bcs)_2]^{3-}$) (Scheme 1). The situation contrasts with the case of $[Cu^{2+}]$ buffered by the couple (Edta′, $[Cu^{II}Edta]^{2-}$) shown in Fig. 1a(i).

For both cases, pM increases with increasing total ligand concentration at a constant total metal concentration. However, the effect is more profound for a 1:2 complex than for a 1:1 complex. Consequently, by varying the concentrations of ligand and metal complex, ligands that form 1:2 complexes are capable of buffering metal concentrations over a wider range than are ligands that form 1:1 complexes (*e.g.*, Fig. 1b).

It must be emphasized that the unit of $(\beta_2')^{-1}$ (M^2) for a 1:2 complex is different from that of $(K_A')^{-1}$ or K_D (M) for a 1:1 complex. It is inadvisable to attempt to compare directly the metal affinities of 1:1 and 1:2 complexes. For example, Edta binds Cu^{II} to form the 1:1 complex $[Cu^{II}(Edta)]^{2-}$ with $K_A = 3.2 \times 10^{15}$ M^{-1} at pH 7.0 while Bcs binds Cu^{I} to produce the 1:2 complex $[Cu^{I}(Bcs)_2]^{3-}$ with $\beta_2 = 6.3 \times 10^{19}$.[11,20] The former value is smaller than the latter value by four orders of magnitude. However, for an occupancy of 50% with each system constrained to produce the same concentration (15 μM) of its metal complex $[Cu^{II}(Edta)]^{2-}$ or $[Cu^{I}(Bcs)_2]^{3-}$, the 'free' metal concentrations $[Cu^{2+}]$ or $[Cu^{+}]$ are calculated to be 3.2×10^{-16} M and 2.6×10^{-16} M, respectively, *i.e.*, they are similar, being close to the cross-over point of lines (i) and (ii) in Fig. 1a. But, the 'free' metal concentration buffered by the 1:2 complex changes much more sensitively with variation of ligand and metal concentrations (Fig. 1).

3 Determination of metal–protein affinities

3.1 General considerations

Affinities are determined *in vitro* and it is assumed that their relative values remain relevant to the very different conditions present in the cytosols of biological cells.[21] This aspect will be tested soon. Families of fluorescent ligand probes of defined affinities are being developed and these will be capable of accessing different pools of available metal ions within cells.[22–26]

Ligands are generally Lewis bases and binding of metal ions alters the pK_a of the ligand atoms at the binding site. Consequently, the metal binding affinity of a synthetic ligand may be determined by competition with protons, as assessed by potentiometric titration (Bjerrum acid–base titration):[27]

$$nH^{+} + ML \rightleftharpoons M + H_nL \quad (4a)$$

$$nH^{+} + ML_2 \rightleftharpoons M + 2H_nL \quad (4b)$$

Since the proton concentration can be determined accurately with a pH electrode, this approach provides reliable metal-binding constants, provided that the ligand pK_a values are known. Some examples include those for various forms of zinquin for Zn^{II},[28] of Par for Zn^{II},[29] of glycine for Cu^{II},[27] and of Bcs and related ligands for Cu^{II}.[11,30,31] However, at present, the approach cannot be applied reliably to proteins. Not only are protein conformations sensitive to pH (especially outside the physiological range) but a number of amino acid sidechains can

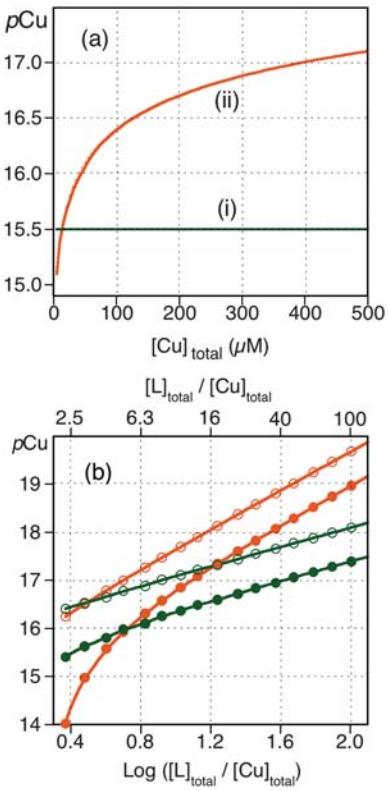

Fig. 1 Metal buffering by couples (Edta′, $[Cu^{II}Edta]^{2-}$) (green traces; based on $K_A = 3.2 \times 10^{15}$ M^{-1} at pH 7.0 from ref. 20) and (Bcs′, $[Cu^{I}(Bcs)_2]^{3-}$) (red traces; based on $\beta_2 = 6.3 \times 10^{19}$ M^{-2} from ref. 11). (a) Theoretical relationships at 50% occupancy. (i) pCu^{2+} *vs.* $[Cu^{II}]_{total}$ under the constraint that $Edta:Cu^{II} = 2.0$; (ii) pCu^{+} *vs.* $[Cu^{I}]_{total}$ under the constraint that $Bcs:Cu^{I} = 4.0$. (b) Metal buffering ranges as a function of $\log([L]_{total}/[Cu]_{total})$ at $[Cu]_{total} = 15$ μM. Empty and filled circles indicate that 20% and 100% of total Cu is bound by ligand.

act as pH buffers, masking the competition between protons and the metal ion for the metal binding site. Consequently, it is usually necessary to estimate metal affinities of proteins by the direct approach of measuring changes in bio-physical properties upon metal binding or by indirect approaches based on competition with suitable probe metals or ligands.

3.2 Direct methods

This normally relies on eqn (1) being a true equilibrium with detectable concentrations of each member of the equilibrium. If the concentration of any one of those species can be determined accurately, the equilibrium concentrations of the others may be deduced by mass balance from the known total concentrations. The estimate of K_D may be calculated from eqn (1) or from a curve-fitting analysis of a series of experimental data *via* eqn (5) (derived from eqn (1)):[32]

$$\theta = [M]/(K_D + [M]) \quad (5)$$

where θ is the metal occupancy of protein P (*i.e.*, $[MP]/[P]_{total}$). In practice, eqn (5) is often converted to more convenient forms with θ being expressed directly as a measurable parameter to facilitate curve-fitting; *e.g.*, see eqn (31) in Section 4.6. However, the sensitivity of direct detection of most convenient quantitative assay methods for metal and protein concentrations is in the micromolar range. At such relatively high concentrations, proteins with significant affinity ($K_D < 10^{-7}$ M) will be saturated and so a true equilibrium is not present.[16] Then the derived K_D value is an upper limit. In fact, many literature values of $\sim 10^{-6}$ M were derived under such conditions, which impose an estimate which is approximately the concentration of protein used in the experiment (*e.g.*, eqn (5) implies that $K_D = [M] \sim [MP]$ for 50% occupancy). It is pertinent that the surfaces of proteins are defined by the sidechains of amino acids which abound with good metal ligands. Adventitious binding of metal ions to protein surfaces is common with K_D values as small as 10^{-6} M. So it is unlikely that a protein that selects for a given metal ion will have such a low affinity.

For high affinity binding, the left-hand side of reaction (1) is favoured, and detection of 'free' metal and protein ligand concentrations is problematical. Mass spectrometry, particularly the application of the electrospray ionisation technique, has been used to estimate metal–protein affinities. While progress has been made in minimising non-specific interactions,[33,34] the question of whether the gas-phase speciation reflects the solution speciation has not been resolved adequately. This is exacerbated when ligand competition is needed to quantify high affinity binding. In the absence of a competing ligand, the same issues of binding saturation arise as those canvassed above. Consequently, the direct approach has limited application. However, if the protein is involved in an effective competition for the metal ion M with a ligand L, then the 'free' metal concentration [M] at much lower than micromolar concentrations may be obtained from a competition relationship such as eqn (9) and then the K_D value from eqn (5). This is discussed in Section 3.3 and examples are given in Section 4.6.

Isothermal titration calorimetry (ITC) detects the change in heat content upon titration of metal ion into *apo*-protein solution and so, in principle, can be applied.[35,36] However, the observed change can include contributions from associated equilibria and so careful assessments of the influence of redox, precipitation and hydrolysis equilibria plus the metal and proton binding capacities of the buffer must be included. These aspects can lead to significant error in estimates of K_D. Ref. 36 discusses these challenges in detail.

3.3 Equilibrium competition methods

The types of reactions which can be probed include competition between (i) two metals for the same protein ligand and (ii) two ligands for the same metal.

3.3.1 Competition between two metal ions for the same protein ligand. Such competition is based on the following general reaction with limiting protein and an excess of each metal ion M and M′:

$$M' + M\text{–}P \rightleftharpoons M'\text{–}P + M \quad (6)$$

The protein components may be separated from excess metal ions and analysed for metal content, providing a qualitative

comparison of the relative affinities. Such a comparison is based on the following assumptions: (i) the metals bind competitively at the same binding site; (ii) the excess 'free' metal ions do not hydrolyse significantly. These assumptions are not always viable. Thus, application of this approach is limited.

A special form of the competition in eqn (6) involves protons according to eqns (4a) and (4b). This forms the basis of reliable potentiometric titration for determination of binding constants of small synthetic ligands.[37] However, as discussed in Section 3.1, the approach is not suitable for proteins.

3.3.2 Competition between two ligands for the same metal ion. A typical situation is described by eqn (7) and (8) where (i) the metal ion concentration is limiting and (ii) ligand L is bi- or multi-dentate:

$$MP + L' \rightleftharpoons ML + P \quad K_{ex7} \tag{7}$$

$$MP + 2L' \rightleftharpoons ML_2 + P \quad K_{ex8} \tag{8}$$

This method appears to provide the most reliable estimates, provided that the affinity standards are accurate and effective competition can be established and quantified. The approach relies solely on the *final equilibrium positions* of competitions (7) and (8) and is not affected by the process of complex formation. The concentration of 'free' metal ion M is usually very low at equilibrium. Potential problems of metal hydrolysis and of metal ions bound by weak ligands such as by pH buffers and Cl^- will be suppressed and usually can be ignored (see Section 3.3.3 below). While it would be possible to probe reactions (7) and (8) by ITC, the usual approach measures the heat change for reactions (1)–(3) directly, and initial metal speciation such as binding by ligands besides water (*e.g.*, Cl^-, pH buffers, *etc.*) will affect the experimental outcomes.

To ensure effective competitions in reactions (7) and (8), the competing ligand L must be in excess and, depending on the pK_a of the ligand and the pH of the reaction medium, competitive binding of protons may need to be considered (see Section 3.3.6). Thus L′ in eqns (7) and (8) refers to all forms of the ligand (usually different protonation states) that are not bound to metal ion M. In addition, if eqns (7) and (8) involve low affinity ligands L, then competition from pH buffers and other weak ligands may still influence the results significantly. In such cases, the weak ligands must be avoided or their contributions to metal speciation at equilibrium must be assessed carefully and kept under control (see Section 4.5).

While ternary complexes L–M–P will almost certainly be intermediates in the establishment of equilibria (7) and (8), it is important to demonstrate that they do not contribute significantly to those equilibria. This may be tested by varying the metal occupancies on both competing ligands and ensuring (i) that spectroscopic probes of concentration vary in intensity only and (ii) that a consistent K_D can be derived under those varying occupancies.

3.3.3 Competition with ligands that form both 1:1 and 1:2 complexes. The metal speciation for equilibria 7 and 8 may be analysed as follows, assuming negligible contributions from low affinity ligands (*e.g.*, pH buffer) and from metal ion hydrolysis:

$$\begin{aligned}[M]_{total} &= [MP] + [M] + [ML] + [ML_2] \\ &= [MP] + [M] + K'_{A1}[M][L'] + K'_{A1}K'_{A2}[M][L']^2 \\ i.e.,\ [M] &= ([M]_{total} - [MP]) / \left(1 + K'_{A1}[L'] + K'_{A1}K'_{A2}[L']^2\right) \\ &= ([M]_{total} - [MP]) / \left(1 + K'_{A1}[L'] + \beta'_2[L']^2\right)\end{aligned} \tag{9}$$

$$[L'] = [L]_{total} - [ML] - 2[ML_2] \tag{10}$$

where [M] is the 'free' metal concentration and [L′] is the total concentration of free ligand which does not bind metal. Parameters K_{A1}', K_{A2}' and β_2' are defined in eqns (2) and (3).

The term $(1 + K_{A1}'[L'] + K_{A1}'K_{A2}'[L']^2)$ in eqn (9) represents the relative contributions of M, ML and ML_2 to metal speciation. If L is in excess with $[L'] \geq 10^{-5}$ M at equilibrium and if $K_{A1}' \geq 10^7\ M^{-1}$, then $K_{A1}'[L'] \geq 100 \gg 1$ and the contribution of [M] can be ignored. Likewise, the relative contribution of ML and ML_2 can be assessed by the relationship $[ML_2]/[ML] = K_{A2}'[L']$ and if $K_{A2}' \geq 10^7\ M^{-1}$, then $[ML_2] \geq 100\,[ML] \gg [M]$ and the contributions of both M and ML can be ignored. These two cases will be assessed separately in Sections 3.3.4 and 3.3.5.

If $K_{A1}' < 10^7\ M^{-1}$ and $K_{A2}' < 10^7\ M^{-1}$, the contributions of all three metal species, M, ML and ML_2, may need to be considered *via* eqns (9) and (10). Then, the affinity of protein P for metal M may be obtained from eqns (9) and (10) under the condition of $[MP] = 0.5\,[P]_{total}$ since, by definition of eqn (1), K_D equals the 'free' metal concentration [M] at 50% metal occupancy of the protein. Examples are given in Sections 4.3.4 and 4.5. Alternatively, K_D may be estimated (probably more adequately) by a curve-fitting of the experimental data to eqn (5), and selected examples are given in Section 4.6.

3.3.4 Competition with ligands that form 1:1 complexes. To ensure effective competition of eqns (7) and (8), [L′] must be usually maintained at $\geq 10^{-5}$ M for detection by most laboratory instruments. If ligand L forms a 1:1 complex ML with high affinity ($K_A' > 10^7\ M^{-1}$) and if the concentration of 1:2 complex ML_2 is negligible (*i.e.*, $K_{A2}' \ll 10^7\ M^{-1}$), the following relationships hold: $[M]_{total} - [MP] \approx [ML]$ and $1 + K_{A1}'[L'] + \beta_2'[L']^2 \approx K_{A1}'[L']$. Then, eqn (9) confirms that exchange reaction (7) only is relevant and provides the 'free' metal concentration [M] *via* eqn (2) and consequently K_D *via* eqn (1) (or its equivalent, eqn (5)). Alternatively, eqn (11) is derived from a combination of eqns (1), (2) and (7).

$$K_{ex7} = \left(\frac{[M][P]}{[MP]}\right)\left(\frac{[ML]}{[M][L']}\right) = K_D K'_A \tag{11}$$

It can also be transformed into eqn (14) *via* the mass balance relationships of eqns (12) and (13):

$$[P] = [P]_{total} - [MP] \tag{12}$$

$$[L'] = [L]_{total} - [ML] \tag{13}$$

$$K_D K_A' = \frac{([P]_{total}/[MP]) - 1}{([L]_{total}/[ML]) - 1} \quad (14)$$

If the equilibrium concentration of any single species in reaction (7) can be determined experimentally and the total concentrations of M, P and L are known, the equilibrium concentrations of all species can be calculated from the mass balance. Then, K_D may be calculated from either eqn (11) or eqn (14). It follows from eqn (14) that the conditions $[P]_{total} > [MP]$ and $[L]_{total} > [ML]$ must both be satisfied for exchange reaction (7) to be an effective competition. Then, a plot of $(([P]_{total}/[MP]) - 1)$ *versus* $(([L]_{total}/[ML]) - 1)$ will generate a straight line with slope equal to $K_D K_A'$. Equivalently, $K_D K_A'$ may also be obtained from a curve-fitting of a series of experimental data to eqn (14). Note that eqns (11) and (14) were derived with the assumption that ternary complexes P–M–L do not contribute to the equilibrium. Their influence can be discounted if conditions (i) and (ii) discussed in Section 3.3.2 are met. Several examples of this approach are given in Section 4.3.

3.3.5 Competition with ligands that form 1:2 complexes. As discussed in Section 3.3.3, if $K_{A2}' \geq 10^7\ M^{-1}$, then a free ligand concentration of $[L'] \geq 10^{-5}$ M is high enough to suppress the contribution of ML to < 1% ML_2. Under such conditions, $[M]_{total} - [MP] \approx [ML_2]$ and $1 + K_{A1}'[L'] + \beta_2'[L']^2 \approx \beta_2'[L']^2$ and hence exchange reaction (8) only is relevant and eqn (9) simplifies to eqn (3). This provides the 'free' metal concentration [M] and also K_D *via* eqn (1) or eqn (5). Alternatively, K_D may be calculated directly from the derived relationships eqns (15) or (17) without the need to calculate [M].

$$K_{ex8} = \left(\frac{[M][P]}{[MP]}\right)\left(\frac{[ML_2]}{[M][L']^2}\right) = K_D \beta_2' \quad (15)$$

$$[L'] = ([L]_{total} - 2[ML_2]) \quad (16)$$

$$K_D \beta_2' = \frac{([P]_{total}/[MP]) - 1}{\{([L]_{total}/[ML_2]) - 2\}^2 [ML_2]} \quad (17)$$

Transformation of eqn (15) to eqn (17) is based on the mass balances of eqns (12) and (16). If several sets of experimental data are available, then an average $K_D\beta_2'$ value should be derived by a global optimal curve-fitting of all the data to eqn (17). Note the validity of eqns (15) and (17) is based on two assumptions: (i) the concentrations of ternary complexes P–M–L are negligible; (ii) the 1:2 complex ML_2 dominates with negligible contribution from the 1:1 complex ML. Selected examples of this approach are given in Section 4.4.

3.3.6 Ligand protonation and apparent binding affinity. It must be emphasized again that L′ in the above discussion refers to all forms of ligand L that do not bind metal ion M (eqns (10), (13) and (16)) and so K_A' and β_2' are the corresponding apparent association constants of the complexes ML and ML_2, respectively. For high affinity binding under the condition of excess ligand, $[M]_{free}$ is low, and so weak effects including metal ion hydrolysis are suppressed and do not generally need to be considered. However, excess ligand is often subject to proton competition *via* eqns (4a) or (4b) which are effectively combinations of eqns (2) and (18) or eqns (3) and (18).

$$L + nH \rightleftharpoons H_nL \quad \beta_{H,n} = [H_nL]/([L][H]^n) \quad (18)$$

$\beta_{H,n}$ is defined as the accumulated protonation constant of H_nL. Eqn (19) follows from the mass balance.

$$[L]_{total} = [ML] + [L] + [HL] + [H_2L] + \ldots + [H_nL] \quad (19)$$

Therefore, for 1:1 complexes, [L′] as given by eqn (20) can be derived from eqns (13), (18) and (19). Then eqn (21) between the apparent association constant K_A' and the pH-independent absolute association constant K_A follows from eqns (2) and (20).

$$[L'] = [L]_{total} - [ML] = [L]/\alpha_{H-L} \quad (20)$$

$$K_A' = \frac{[ML]\alpha_{H-L}}{[M][L]} = K_A \alpha_{H-L} \quad (21)$$

[L] is the concentration of deprotonated ligand defined in eqns (18) and (19) and α_{H-L} is Schwarzenbach's α-coefficient which can be calculated theoretically for any given pH from eqn (22):[38]

$$\begin{aligned} \alpha_{H-L} &= \left(1 + \beta_{H,1}[H] + \beta_{H,2}[H]^2 + \ldots + \beta_{H,n}[H]^n\right)^{-1} \\ &= \left(1 + \sum \beta_{H,n}\,[H]^n\right)^{-1} \end{aligned} \quad (22)$$

For 1:2 complexes, the equivalent relationship is eqn (23).

$$\beta_2' = \frac{[ML_2](\alpha_{H-L})^2}{[M][L]^2} = \beta_2(\alpha_{H-L})^2 \quad (23)$$

For those ligands with high pK_a in a medium of low pH, $\sum\beta_{H,n}[H]^n \gg 1$ and $\alpha_{H-L} \ll 1$, so $K_A' \ll K_A$ and $\beta_2' \ll \beta_2$. Consequently, the effect of protonation is significant, particularly for β_2'. On the other hand, for those ligands with low pK_a in a medium of high pH, $\sum\beta_{H,n}[H]^n \ll 1$ and $\alpha_{H-L} \sim 1$, so $K_A' \sim K_A$ and $\beta_2' \sim \beta_2$. Then the effect of protonation is minimal (Tables 1 and 2).

3.3.7 Ligands that form 1:1 complexes. A list of non-chromophoric ligands based upon amine carboxylates is given in Table 1 with structures in Scheme 1. These ligands are multidentate chelators and usually react with metal ions to form stable 1:1 complexes ML ($K_A > 10^7\ M^{-1}$) with little tendency to form stable 1:2 complexes ML_2 or ternary complexes P–M–L. Thus, competition for metal M between these ligands and proteins is usually analysed *via* eqn (7), (11) and (14), as discussed in Section 3.3.4. However, due to the amine functionalities, these ligands usually exhibit high pK_a values. Consequently, their α_{H-L} coefficients are small and their metal-binding affinities are pH-dependant and may not satisfy the condition of $K_A' > 10^7\ M^{-1}$ at lower pH (Table 1). In such cases, the analysis may need to be performed with more general eqn (9) and (10). Note that the formation constants for the divalent first-row transition metal ions in Table 1 obey the Irving–Williams series.[42]

Tpen is a neutral pyridyl-amine ligand (Scheme 1) with advantages of membrane permeability and low pK_a values (K_D less pH-dependent; Table 1). Note that its formation constants

Table 1 Absolute formation constants ($\log K_A$) of complexes ML in solutions of ionic strength 0.1 M.[a]

	Cdta	Edta	Egta	Hedta	Nta	Tpen	BisTis [b]	Mf2 [c]
HL/H L [d]	12.3	10.19	9.40	9.87	9.73	7.12	6.56	—
H_2L/H HL [d]	6.11	6.13	8.79	5.38	2.49	4.81	—	—
H_3L/H H_2L [d]	3.50	2.69	2.70	2.62	1.89	3.30	—	—
H_4L/H H_3L [d]	2.48	2.00	1.9	—	—	2.88	—	—
α (pH 7.0) [e]	4.4×10^{-6}	5.7×10^{-4}	6.4×10^{-5}	1.3×10^{-3}	1.9×10^{-3}	0.43	0.73	—
Mn^{II}	17.5	13.9	12.2	11.1	7.27	10.13	0.70	—
Fe^{II}	18.9	14.3	11.8	12.2	8.90	14.38	—	—
Fe^{III}	30.0	25.1	20.5	19.7	16.0	—	—	—
Co^{II}	19.7	16.45	12.3	14.5	10.38	16.4	1.78	—
Ni^{II}	20.2	18.4	13.5	17.1	11.51	21.3	3.59	—
Cu^{II}	22.0	18.78	17.7	17.4	13.0	20.2	5.27	—
Zn^{II}	19.3	16.5	12.6	14.6	10.66	15.4	2.38	7.7
Cd^{II}	19.7	16.5	16.5	13.7	9.76	16.09	2.47	—

[a] From ref. 20 except those indicated. [b] From ref. 39. [c] From ref. 40. [d] Refers to the indicated protonic equilibrium. [e] Calculated *via* eqn (22).

for the divalent first row transition metal ions do not follow the Irving–Williams series strictly and peak at Ni^{II} rather than Cu^{II} (Table 1). The likely reason is that the ligand binds Cu^{II} as a pentadentate ligand but as a hexadentate ligand for the other metal ions.[43]

Mag-fura-2 (Mf2; Scheme 1) is a popular chromophoric ligand that has been employed widely to quantify Zn^{II} binding in proteins. Upon reaction with excess Zn^{2+}, the intense absorbance at 366 nm (ε, 2.99×10^4 M^{-1} cm^{-1}) characteristic of the free ligand shifts to 325 nm and there is a low residual absorbance only at 366 nm (ε, 1.88×10^3 M^{-1} cm^{-1}) (Fig. 2a). Two tight isosbestic points are seen at 342 and 276 nm, consistent with a clean 1:1 reaction. The binding affinity is in the nanomolar range (K_D, 2.0×10^{-8} M) and does not seem to be dependent on pH within the range pH 7.0–7.8 (due, presumably, to low pK_a values of the carboxylate ligands; see Scheme 1 and Table 1).[40] This suggests that Mf2 is a sensitive probe for quantification of Zn^{II} binding of proteins with similar affinities. However, application of this probe is hindered by the narrow metal-buffering range (Fig. 2c, green traces[15]). This limitation is imposed by an experimental detection limit of ~35 μM for the total Mf2 concentration as the probe detects Zn^{II} binding indirectly *via* the absorbance of the free ligand. A new water-soluble bis(thiosemicarbazone) ligand detects Zn^{II} binding directly and shows promise as a replacement for Mf2.[44]

3.3.8 Ligands that form both 1:1 and 1:2 complexes. These ligands are generally bidentate with relatively small formation constants. A representative example is the non-chromophoric ligand glycine (Gly) which reacts with Cu^{II} with $\log K_{A1} = 8.3$ and $\log K_{A2} = 6.9$ (Table 2).[27] But the coefficient α_{H-L} is small (5.7×10^{-3} at pH 7.4) and so the apparent formation constants are pH-dependant: at pH 7.4, $\log K_{A1}' = 6.0$ and $\log K_{A2}' = 4.6$. Consequently, the optimal Cu^{2+}-buffering range for Gly is $\geq 10^{-9}$ M. It is a popular probe for estimation of the binding affinities of weak Cu^{II}-binding systems such as prion proteins and amyloid-β peptides (Aβ) of Alzheimer's disease.[5–9,45–47] However, the estimation is complicated by the fact that the formation constants are too small to satisfy the requirements for a simple competition relationship *via* either eqn (7) or eqn (8) at most practical ligand concentrations (μM–mM). For example, as $[ML_2]/[ML] = K_{A2}'[L']$, and at pH 7.4, $K_{A2}' = 10^{4.6}$ so when $[L'] = 10^{-4.6}$ M (*i.e.*, 25 μM), and the concentrations of the 1:1 and 1:2 complexes will be equal at equilibrium. At lower pH, the magnitude of [L′] required to maintain these equal concentrations will be higher. Consequently, the data must be analysed *via*

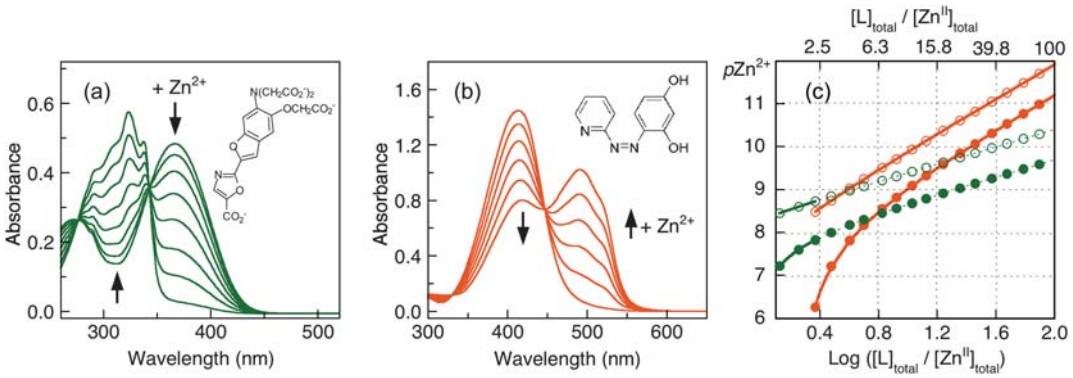

Fig. 2 Properties of Zn^{2+} buffers Mf2 (green) and Par (red) in Mops buffer (50 mM; pH 7.3). (a) Change in solution spectrum of Mf2 (15 μM) upon titration with Zn^{2+} (0.2 mM). (b) Change in solution spectrum of Par (100 μM) upon titration with Zn^{2+} (0.5 mM). (c) Zn^{2+} buffering ranges as a function of log ($[L]_{total}/[Zn]_{total}$) at $[Zn]_{total} = 15$ μM. Empty and filled circles indicate that 20% and 100% of total Zn is bound by the ligand. The plots were calculated based on $K_A = 4.9 \times 10^7$ M^{-1} for Zn^{II}–Mf2 from ref. 40) and $\beta_2 \sim 10^{12}$ at pH 7.3 for $Zn^{II}(Par)_2$ from ref. 15.

Table 2 Absolute formation constants ($\log K_{A1}$, $\log K_{A2}$ and $\log\beta_2$) in solutions of ionic strength 0.1 M

		Gly	Nec		Bcs	Bq [b]	Bca		Par
HL/H L		9.64	5.88	5.79	5.7	3.1	—	—	12.4
H_2L/H HL		2.41	—	—	—	—	—	—	7.0
α_{H-L} [a]		2.3×10^{-3}	0.93	0.94	0.95	1.0	—	—	4.0×10^{-6}
Cu^{I}	$\log\beta_2$	—	19.1	19.5	19.8	~16.5	17.2	14.7	—
Cu^{II}	$\log K_{A1}$	8.27	~6.1	6.2	6.1	4.27	—	—	16.5
	$\log K_{A2}$	6.88	~5.6	5.5	5.8	3.46	—	—	—
	$\log\beta_2$	15.15	~11.7	11.7	11.9	7.73	—	—	—
Zn^{II}	$\log K_{A1}$	—	—	3.4	—	—	—	—	12.4
	$\log K_{A2}$	—	—	4.4	—	—	—	—	11.1
	$\log\beta_2$	—	—	7.8	—	—	—	—	23.5
Ref.		27	30	31	11	30	41	12	29

[a] Calculated *via* eqn (22) for pH 7.0. [b] 2,2-Biquinolyl, data obtained in 50% dioxane–water.

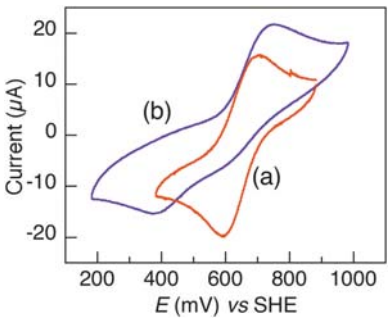

Fig. 3 Comparison of cyclic voltammograms of (a) $[Cu^{I}(Bcs)_2]^{3-}$ (1.0 mM) and (b) $[Cu^{I}(Bca)_2]^{3-}$ (1.0 mM) in KPi buffer (20 mM, pH 7.0; NaCl, 100 mM) at a scan rate of 20 mV s^{-1}. Reproduced, with permission, from ref. 49.

eqns (9) and (10). In addition, weak binding from pH buffers and formation of ternary complexes P–M–Gly may also complicate the system. Some examples of this type of competition are given in Section 4.5.

3.3.9 Ligands that form 1:2 complexes. The other bidentate ligands listed with Gly in Table 2 form complexes with Cu^{I}, Cu^{II} or Zn^{II} and display intense absorbance in the visible region. These ligands are potential chromophoric probes for these metal ions. Their formation constants are usually large enough to allow analysis competition *via* eqns (8), (15) and (17), as discussed in Section 3.3.5.

Ligands Nec and Bcs are derivatives of phenanthroline (Scheme 1; Table 2). They exhibit low pK_a values (4–6)[48] and hence their reactions with metal ions are essentially pH-independant at pH $\geq$ 7 (see α_{H-L} values in Table 2). They react with Cu^{I} and Cu^{II} to form 1:2 complexes. The presence of methyl groups at the 2- and 9-positions provides steric hindrance at the coordination site which favours Cu^{I} binding (tetrahedral preference) over Cu^{II} binding (square planar preference). Consequently, the reduction potentials of the redox couple Cu^{II}/Cu^{I} of these ligands are positive at ~0.62 V *vs.* SHE and the Cu^{I} complexes are stable. However, the intrinsic instability of 'free' Cu^{+} in aqueous solution (disproportionation) prevents determination of the formation constants of $[Cu^{I}(Nec)_2]^{+}$ and $[Cu^{I}(Bcs)_2]^{3-}$ by potentiometric titration. Fortunately, the respective Cu^{II}/Cu^{I} couples are chemically reversible, allowing accurate estimation of their reduction potentials (*e.g.*, Fig. 3a).[49,50] Consequently, β_2 values of the Cu^{I} complexes were estimated *via* the Nernst relationship from the β_2 values of the respective Cu^{II} complexes which, in turn, were determined by reliable potentiometric titration (Table 2).[11,30,31] The affinities of these ligands for Cu^{I} are very high ($\beta_2 \sim 10^{19}$ M^{-2}) and are much higher than those for Cu^{II} ($\beta_2 \sim 10^{12}$ M^{-2}; Table 2).[11,30,31] Introduction of two sulfonated phenyl groups at the 4- and 7-positions improves the water-solubility of ligand Bcs but has little effect on the affinity (Table 2).

The two ligands Bq and Bca are derivatives of 2,2′-bipyridyl (Scheme 1) with ligand properties similar to those of Nec and Bcs (Table 2; pK_a, 3–4[48]). However, Bq is barely water-soluble. Its affinity for Cu^{II} is low ($\beta_2 = 10^{7.7}$ M^{-2}), as determined by potentiometric titration in a mixed solvent of dioxan:water = 1:1.[30] Its affinity for Cu^{I} is much higher ($\beta_2 \sim 10^{16.5}$ M^{-2}), consistent with the observed positive reduction potential of ~ 0.77 V *vs.* SHE for the couple $[Cu^{II}(Bq)_2]^{2+}/[Cu^{I}(Bq)_2]^{+}$ in the mixed solvent.[30] Introduction of two carboxylate groups at the 4- and 4′-positions converts Bq into water-soluble Bca (Scheme 1). However, this modification makes it difficult to estimate the affinities for Cu^{II} *via* the conventional potentiometric approach due to the similar pK_a values of the carboxylates. In addition, although the reduction potential for the couple $[Cu^{II}(Bca)_2]^{2-}/[Cu^{I}(Bca)_2]^{3-}$ in aqueous buffer may be even more positive than the equivalent couple of Bcs, the redox process is irreversible (Fig. 3b[49]), preventing derivation of β_2 for $[Cu^{I}(Bca)_2]^{3-}$ *via* the Nernst equation.

Nevertheless, the formation constant β_2 for $[Cu^{I}(Bca)_2]^{3-}$ has been determined by two independent approaches providing estimates which differ by 2.5 orders of magnitude ($10^{14.7}$ *versus* $10^{17.2}$ M^{-2}; Table 2).[12,41] The latter value was obtained by indirect competition for Cu^{I} between ligands Bca and Bcs ($\beta_2 = 10^{19.8}$ M^{-2}) mediated separately by three *apo* proteins that bind Cu^{I} with different affinities (Atx1, nA-PcoC and C42S-rubredoxin).[41] This estimate is supported by two independent determinations employing the same competition mediated by the CopZ protein from *Bacillus subtilis* and by a protein variant of a Cu^{I} sensor CsoR from *Mycobacterium tuberculosis*.[14,51] Its magnitude of $10^{17.2}$ M^{-2} is comparable to that estimated previously for $[Cu^{I}(Bq)_2]^{+}$ ($\beta_2 \sim 10^{16.5}$ M^{-2}).[30] The second estimate was obtained by ITC *via* titration of a Cu^{+} solution with Bca.[12] The Cu^{+} solution was generated by reduction of Cu^{2+} with ascorbate in NaCl (200 mM) which stabilizes Cu^{+} as $[Cu^{I}Cl_n]^{(1-n)-}$. Titration with Bca would involve a conversion of these species to $[Cu^{I}(Bca)_2]^{3-}$, diminishing the observed heat release relative to conversion from Cu^{+}_{aq}. The two estimates emphasise the strong affinity of Bca for Cu^{I}. The value of $10^{17.2}$ M^{-2} is preferred here as it more closely matches that of $[Cu^{I}(Bq)_2]^{+}$ and leads to a more consistent interpretation of the chemistry of proteins CopK, CopC and PcoC (see Sections 4.4.1 and 4.4.3).

Titration of ligands L (L = Bca or Bcs) with $[Cu^{I}(MeCN)_4]^{+}$ or with Cu^{2+} in the presence of reductants such as ascorbate and NH_2OH induces intense absorbance in the visible region (Fig. 4a), characteristic of complexes $[Cu^{I}L_2]^{3-}$ (L = Bca: λ_{max} = 562 nm,

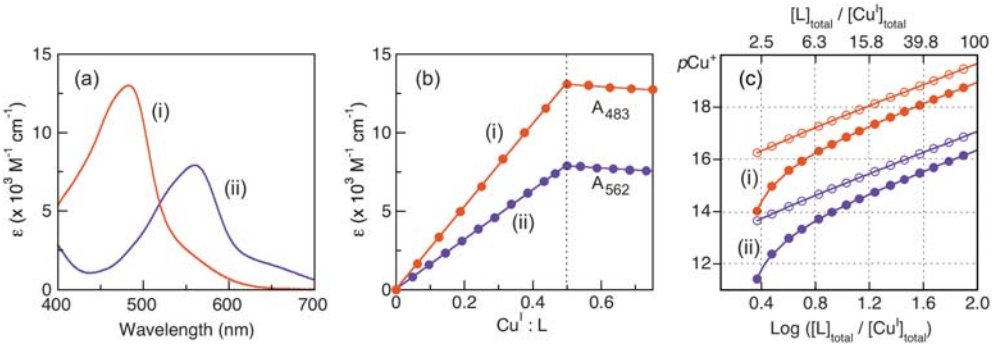

Fig. 4 (a) Solution spectra of $[Cu^{I}L_2]^{3-}$ (40 μM) in Mops buffer (50 mM, pH 7.0): (i) L = Bcs (red); (ii) L = Bca (purple). (b) Change in absorbance upon titration of ligand L (80 μM) upon titration with $[Cu^{I}(MeCN)_4]^{+}$: (i) L = Bcs at $\lambda_{max} = 483$ nm; (ii) L = Bca at $\lambda_{max} = 562$ nm. (c) pCu^{+} buffer ranges for (i) ligand Bcs ($\beta_2 = 6.3 \times 10^{19}$ M^{-2} from ref. 11) and (ii) ligand Bca ($\beta_2 = 1.6 \times 10^{17}$ M^{-2} from ref. 41) upon variation of ligand concentrations with a fixed total concentration of 15 μM for Cu^{I}. Empty and filled circles indicate that 20% and 100% of total Cu^{I} is bound by the ligand.

$\varepsilon = 7900$ M^{-1} cm^{-1}; L = Bcs: $\lambda_{max} = 483$ nm, $\varepsilon = 13\,000$ M^{-1} cm^{-1}).[11,52] The absorbance increases are linear with sharp turning points at $[Cu^{I}]$:[L] = 0.5 (Fig. 4b), indicating clean reactions to produce $[Cu^{I}L_2]^{3-}$ in the presence of excess each ligand. There appears to be little contribution from the 1:1 complexes $[Cu^{I}L]^{-}$ (assuming that their molar absorptivities are different). This is consistent with the high formation constants of these 1:2 complex anions ($\beta_2 > 10^{14}$ M^{-2}). Assuming that $\log K_{A1} \sim \log K_{A2}$ (often the case for 1:2 complexes, see Table 2), then $\beta_2 > 10^{14}$ M^{-2} would suggest $K_{A2} > 10^{7}$ M^{-1} which is sufficient to suppress the formation of the 1:1 complexes in the presence of excess ligand at concentrations $\geq 10^{-5}$ M (*i.e.*, $1 \ll K_{A1}'[L'] \ll \beta_2'[L']^2$ in eqn (9)).

Purified samples of the colourless salt $[Cu^{I}(CH_3CN)_4]ClO_4$ can be used as a reliable primary Cu standard. An alternative is the copper atomic absorption standard solution provided by Aldrich. In addition, the properties of Bca and Bcs discussed above provide a convenient calibration of ligand concentration *via* a copper standard solution (Fig. 4b).[52] The extinction coefficients characteristic for $[Cu^{I}(Bca)_2]^{3-}$ at 562 nm and for $[Cu^{I}(Bcs)_2]^{3-}$ at 483 nm may vary slightly (<5%) with solution composition and with ionic strength, in particular. With Cu-free Bca solution as background, $[Cu^{I}(Bca)_2]^{3-}$ may also be quantified at 358 nm with a five-fold increase in sensitivity ($\varepsilon_{358} = 42\,900$ M^{-1} cm^{-1}; see Fig. 12b).[52] It should be noted that typical purities of these ligands sourced from Sigma are 80–86% for Na_2Bcs and ~95% for Na_2Bca.

Bca and Bcs can also serve as versatile Cu^{+} buffers and probes in the study of copper biology. Bca has been applied commercially in the colorimetric determination of protein concentration, detecting Cu^{+} generated by the biuret reaction while Bcs has been employed widely in depleting copper in biological systems. The 'free' Cu^{+} concentrations buffered by Bca and Bcs may be calculated from $[Cu^{+}] = ([Cu^{I}L_2]/[L]^2)(\beta_2')^{-1}$ (eqn (3)) and so is dependent on both $[Cu^{I}L_2]$ and [L]. As a metal buffer, concentrations of $[Cu^{I}L_2]^{3-}$ are usually controlled in the range 10–50 μM, correlating to $[Cu^{+}]$ concentrations in the range $0.3–1.6 \times 10^{-13}$ M for L = Bca and $0.8–4.0 \times 10^{-16}$ M for L = Bcs, assuming that 50% of ligand L binds Cu^{I} and 50% is unbound. In practice, these buffer ranges may be extended further by variation of the total concentration ratio of $[L]_{total}/[Cu^{+}]_{total}$ (Fig. 4c). Some examples are given in Section 4.4.

The bidentate ligand Par is a popular Zn^{2+} probe (Scheme 1). It normally acts as a tridentate ligand *via* its azo, pyridyl and 3-hydroxyl functions.[29] Binding is detected from the absorbance of the 1:2 complex rather than that of the free ligand ($\varepsilon_{500} \sim 80\,000$ and 1400 M^{-1} cm^{-1} for the complex and the ligand, respectively; Fig. 2b). Consequently, it has the advantage of a much wider Zn^{2+} buffering range than Mf2 (Fig. 2c) and so is capable of quantifying a wider range of affinities. However, application of Par as a competing ligand is problematical for several reasons. Firstly, it features two ionizable hydroxyl functions and Zn^{II} binding leads to deprotonation of the less acidic 1-hydroxyl ($pK_a = 12.4$) as well as its ligand 3-hydroxyl ($pK_a = 7.0$), imposing a very small α_{H-L} (Table 2).[29] Therefore, the apparent formation constant β_2' is highly pH-dependant and difficult to define accurately (*cf.* eqn (23); Table 3). Secondly, the molar absorptivity ε_{500} of the complex also changes dramatically with pH around 7 due to the equilibria involving the multiple protonation states of the 1:2 complex. The values of pK_{a1} and pK_{a2} for the 1:2 complex were reported to be 7.7 and 9.3 in one study[29] and to be 6.45 and 7.55 in another.[53] Finally, β_2' at pH 7.0 is smaller than the value of 10^{14} M^{-2} which is required to ensure effective competition in reaction (8) and so a relatively high concentration of free ligand must be present to suppress the contribution of the 1:1 complex. These complications have been ignored in a number of studies.[54–57]

Table 3 pH dependence of spectrum and formation constants for the Zn^{II}–Par system

			β_2'/M^{-2}		
pH	λ_{max}/nm	$\varepsilon/10^3$ M^{-1} cm^{-1}	Exptl.	Calc. [b]	Ref.
7.0	500	66.0	2×10^{12}	3.2×10^{12}	59
5.5–7.0	490	70.9	1×10^{13}	—	60
7.3	500	80.0	1.1×10^{12}	1.3×10^{13}	15
8.4	500	89.0	7.7×10^{16}	2.0×10^{15}	15
>9.0	490	92.9	3.2×10^{20}	$>3.2 \times 10^{16}$	60
9	495	95.8	1.6×10^{22}	3.2×10^{16}	53
			2×10^{23} [a]		29

[a] Determined by potentiometric titration. Therefore, this β_2 value is regarded as the absolute formation constant. [b] Calculated *via* eqns (22) and (23).

The above difficulties may be circumvented by calibration of the affinity of Par (L in eqns (7) and (24)) with a spectroscopically silent ligand of known K_A' (such as Egta; Scheme 1).[15,58]

$$\text{Zn–Egta} + 2\text{L}' \rightleftharpoons \text{ZnL}_2 + \text{Egta} \quad K_{ex24} \tag{24}$$

$$K_{ex24} = \beta_2'/K_A' \tag{25}$$

$$K_D = \left(K_A'\right)^{-1} \times \frac{K_{ex7}}{K_{ex24}} \tag{26}$$

The uncertainties associated with β_2' and ε in eqns (15) and (25) are eliminated by performing separate competitions with the target protein (eqn (7)) and with the affinity standard (eqn (24)) in the same reaction buffer while ensuring similar Zn^{II} occupancies on both (see examples in Section 4.4.4).

4 Selected case studies

Rather than to review the literature extensively, the aim here is to survey methods for estimation of the affinities of metalloproteins for their metal ions and to pinpoint potential problems. Representative examples have been selected to illustrate the different cases discussed in Section 3. Our own work is favoured to facilitate the graphical illustrations.

4.1 Direct binding of metal ion to protein ligand

Binding of Co^{2+} to a zinc finger peptide (29-mer) induced changes in solution spectra and so Co^{II} occupancy could be monitored directly.[61] The binding was weak with no clear turning point, implying that eqn (1) was a true equilibrium. Free $Co^{2+}{}_{aq}$ concentrations were obtained directly from the difference between the total concentration of Co^{2+} added and that bound to the peptide (assuming that adventitious binding was absent). A dissociation constant of $K_D = 3.8 \times 10^{-6}$ M was estimated *via* curve-fitting to eqn (5) of data acquired with varying peptide concentration (5–33 μM).[61]

Another example of low affinity binding is the chaperone protein *apo*-CopK. It is a weakly associated dimer and binds Cu^{II} with $K_D \geq 10^{-6}$ M, as detected by both UV-visible and fluorescence probes.[62] The bound Cu^{II} does not cause dimer dissociation and may be removed readily and quantitatively upon buffer change with a desalting column. However, the protein binds Cu^{I} with high affinity, accompanied by dimer dissociation and generation of a high affinity Cu^{II} site of sub-picomolar affinity.[62] More details of this cooperative binding of Cu^{I} and Cu^{II} are given in Sections 4.3 and 4.4.

4.2 Direct competition between metal ions for a protein ligand

These reactions are performed generally with two metals ions in excess and so is frequently complicated by the effects of metal hydrolysis or adventitious binding of the ions to buffers and/or proteins (Section 3.3.2). Consequently, reliable quantitative data can be difficult to extract. However, the relative affinities of different ions for the same site (but not necessarily the identical ligand set) may be estimated this way. For example, the CopC protein from *Pseudomonas syringae* features separate binding sites specific for Cu^{I} and Cu^{II} (Fig. 5a).[63–65] Both empty sites in the *apo*-protein □□–CopC can bind Hg^{2+} to give $Hg^{II}Hg^{II}$–CopC. The specificity of Cu^{I} and Cu^{II} for their respective sites was demonstrated convincingly and conveniently by sequential titration of Cu^{+} and then Cu^{2+} (Fig. 5b) or Cu^{2+} and then Cu^{+} (Fig. 5c) into $Hg^{II}Hg^{II}$–CopC.[64,65] Cu^{+} and Cu^{2+} could each displace one equivalent only of bound Hg^{II}.

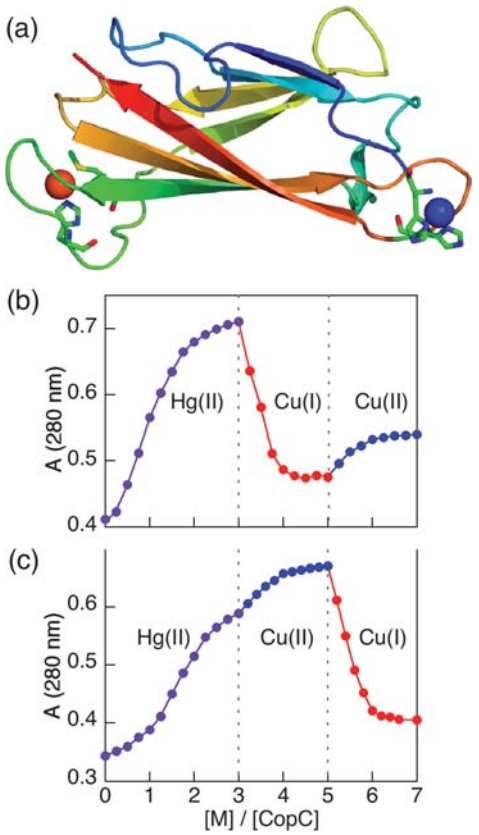

Fig. 5 (a) Ribbon representation of the $Cu^{I}Cu^{II}$–CopC molecule (PDB code: 2C9Q) highlighting two distinct copper sites (Cu^{I} in red and Cu^{II} in blue) and copper ligands (in sticks). (b, c) Changes in absorbance at 280 nm upon sequential titration of *apo*-CopC in Mes buffer (20 mM; pH 6.0) with Hg^{2+} (3 eq), followed by (b) $[Cu(MeCN)_4]^{+}$ (2 eq.) and $Cu^{2+}{}_{aq}$ (2 eq.) or (c) $Cu^{2+}{}_{aq}$ (2 eq.) and $[Cu(MeCN)_4]^{+}$ (2 eq.). Modified from refs. 64 and 65.

In the example described in Section 4.1, Co^{2+} binds weakly to a zinc finger peptide ($K_D = 3.8 \times 10^{-6}$ M) with characteristic absorbance in the UV and visible ranges. Titration of Zn^{2+} into a solution containing the peptide and excess Co^{2+} induced decay of the absorbance intensity, consistent with the presence of equilibrium (27).[32,61] The affinity for Zn^{II} ($K_D \sim 10^{-9}$ M) could then be estimated.[61]

$$\text{P–Co}^{II} + \text{Zn}^{2+}{}_{aq} \rightleftharpoons \text{P–Zn}^{II} + \text{Co}^{2+}{}_{aq} \tag{27}$$

Competition for protein P may also be performed between a metal ion M and a metal complex $M'L_n$ to emphasise large differences in the affinities of protein P for M and M′. For example, the binding affinities of HMA4n (the N-terminal metal binding domain (MBD) of the zinc transporter HMA4 from *Arabidopsis thaliana*) for Cu^{I} and Zn^{II} were estimated by separate ligand competitions involving different chromophoric probes Bca and Par, respectively (see Sections 4.4.3 and 4.4.4). The

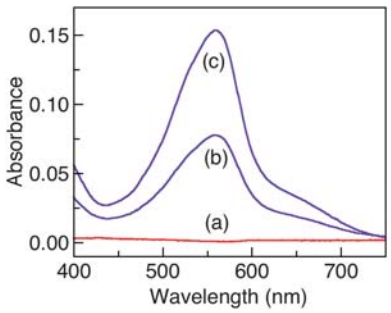

Fig. 6 Solution spectra of a mixture of *apo*-HMA4n (10 μM) and Bca (45 μM) in Mops buffer (50 mM; pH 7.3; 100 mM NaCl) upon addition of (a) 10 μM Cu^{+}; (b) 20 μM Cu^{+}; (c) same as (b) without HMA4n. Spectra were not affected by doubling the concentration of Bca to 90 μM or by addition of Zn^{2+} (20 μM) either before or after the addition of Cu^{+}. Reproduced, with permission, from ref. 15.

affinity for Cu^{I} ($K_D \sim 10^{-17}$ M) was found to be much higher than the affinity for Zn^{II} ($K_D \sim 10^{-10}$ M).[15] In addition, the affinity of Bca for Cu^{I} is much higher than its affinity for Zn^{II}. Direct metal competition experiments were performed in which both Zn_{aq}^{2+} and Cu_{aq}^{+} and then '$[Zn^{II}(Bca)_x]$' (x = 1 and/or 2) and $[Cu^{I}(Bca)_2]^{3-}$ competed for HMA4n. The experiments showed that not only 'free' Cu^{+}, but also Cu^{I} from $[Cu^{I}(Bca)_2]^{3-}$ could displace Zn^{II} quantitatively from Zn^{II}–HMA4n (eqn (28); Fig. 6).[15]

$$Zn^{II}\text{–HMA4n} + [Cu^{I}(Bca)_2]^{3-} \rightarrow Cu^{I}\text{–HMA4n} + '[Zn^{II}(Bca)_x]' \quad (28)$$

When considering the difference in affinities of HMA4n for Cu^{I} and Zn^{II} ($K_D(Cu^{I})/K_D(Zn^{II}) \sim 10^{-7}$), reaction (28) must be partially driven by the formation of the uncharacterised complex(es) '$[Zn^{II}(Bca)_x]$'. However, a control experiment involving competition for Zn^{II} between ligands Bca and Mf2 (Scheme 1) confirmed that Bca buffers free Zn^{2+} at a concentration above 10^{-8} M, much higher than the free Cu^{+} concentration buffered by Bca at $\sim 10^{-13}$ M (see Section 3.3.9). As reaction (28) goes to completion, the affinity of HMA4n for Cu^{I} is confirmed to be much higher than the affinity for Zn^{II}.[15]

4.3 Competition involving 1:1 complexes

Eqns (7), (11) and (14) provide general formulae for competition for a metal ion M between a protein ligand P and a synthetic ligand L which forms a stable 1:1 complex ML. They include consideration of the affinity of the synthetic ligand for protons. The challenges are (i) to establish at least one reliable probe to measure the concentration of one or more of the species in eqn (7); (ii) to ensure that eqn (7) is an *effective* competition with insignificant contribution from ternary complexes (see Section 3.3.4); (iii) to have a reliable affinity standard (Sections 3.3.7–3.3.9; Tables 1 and 2). Representative examples with different strategies to meet these challenges are given in this section.

4.3.1 Affinities of CopC and PcoC for Cu^{II}. PcoC from *E. coli* and CopC from *Pseudomonas syringae* are homologous bacterial periplasmic proteins involved in copper resistance.[66] They exhibit 67% sequence identity and both feature separated metal binding sites specific for Cu^{I} and Cu^{II} (Fig. 5a).[52,63,65,67] The single tryptophan residue located between the two copper binding sites in each protein fluoresces intensely at ~325 nm when excited at 290 nm. Binding of Cu^{II} quenched the fluorescence intensity linearly (Fig. 7a and b(i)), allowing Cu^{II} binding to be monitored quantitatively according to the relationship $[P]_{total}/[CuP] = \Delta F_1/\Delta F_x$, where ΔF_1 and ΔF_x are the changes in fluorescence intensity when PcoC or CopC is loaded with one and x ($x < 1$) equivalent of Cu^{II}, respectively. The second term $[L]_{total}/[CuL]$ in eqn (14) may be obtained from mass balance under the conditions of effective competition (*i.e.*, $[CuL] = [Cu]_{total} - [CuP]$).

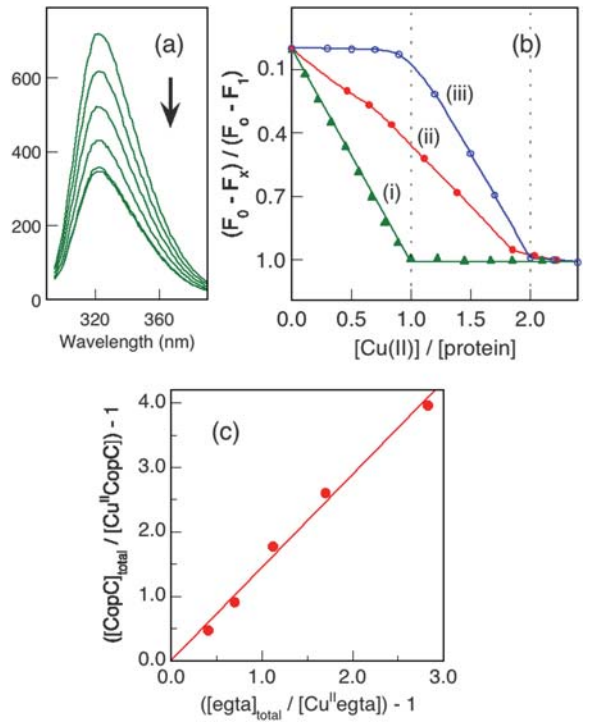

Fig. 7 Determination of Cu^{II} dissociation constants K_D for PcoC proteins (5 mM) in KPi buffer (20 mM; pH 7.0; NaCl, 100 mM). (a) Quenching of fluorescence emission intensity for *apo*-PcoC (□□) upon titration with Cu^{2+} solution (100 μM). (b) Change in fluorescence emission intensity (expressed as Cu^{II} occupancy) as a function of Cu^{II} concentration in the presence of (i) □□; (ii) □□ and Egta (5.0 μM); (iii) □□ and Edta (5.0 μM). (c) Plot of eqn (14) for effective competition for Cu^{II} between □□ and Egta. Reproduced, with permission, from ref. 52.

The *apo*-proteins are represented by □□ to indicate empty Cu^{I} and Cu^{II} binding sites. Titration of □□ (5 μM) with Cu^{2+} quenched the fluorescence intensity linearly with a sharp turning point at $[Cu^{2+}]/[P] = 1.0$ (Fig. 7b(i)). The equivalent titration in the presence of one equivalent of Edta caused no quenching until the latter was effectively saturated (Fig. 7b(iii)). These two experiments provide the two controls of 'no competition' and 'overwhelming competition'. They indicate that K_D for Cu^{II} must be smaller than 10^{-6} M but larger than 3.1×10^{-16} M, the K_D' value for Edta.[20] The same titration in the presence of one equivalent of the weaker Cu^{II} ligand Egta (K_D', 2.5×10^{-14} M)[20] induced fluorescence quenching intermediate between the two previous cases, consistent with an effective competition for Cu^{2+}

between the respective proteins and the ligand Egta (Fig. 7b(ii); eqn (7)). Consequently, the Cu^{II} binding affinities of these two proteins were estimated reliably from eqns (7) and (14) (Fig. 7c) and were found to be indistinguishable.[52,65] This was confirmed independently by direct competition for Cu^{II} between these two proteins.[52]

It must be emphasised that the Cu^{II} exchange rates of reaction (7) may be slow and it is important to perform the same reaction from both directions to ensure that the system has reached the equilibrium.[52] In the above example, the fluorescence of the target proteins acts as a metal binding probe while the synthetic ligand acts as an affinity standard.

4.3.2 Affinity of CopK for Cu^{II}. CopK from the Gram-negative bacterium *Cupriavidus metallidurans* CH34 is another periplasmic copper-binding protein involved in copper resistance.[68] The *apo* form is a weakly associated dimer ($K_D \sim 10^{-5}$ M) with low affinity for Cu^{II} ($K_D > 10^{-6}$ M) but high affinity for Cu^{I} ($K_D \sim 10^{-11}$ M).[62,69] Cu^{I} binding induces dimer dissociation and enhances the Cu^{II} binding affinity by a factor of at least 10^6.[62] However, Cu^{I}–CopK is air-sensitive and it is a difficult challenge to quantify the affinity of Cu^{I}–CopK for Cu^{II} in the necessary absence of reductant. In addition, it was not possible to estimate the Cu^{II} K_D by the approach used for PcoC and CopC (Section 4.3.1), as the fluorescence response of CopK to Cu^{II} binding is weak and cannot be distinguished from the response due to dimer dissociation induced by Cu^{I} binding (Fig. 8a(i,ii) and 8b(i,ii)). However, a CopC variant with its Cu^{I} site disabled (⊠□–CopC) exhibits an intense fluorescence response to Cu^{II} binding (Fig. 8a(iii, iv); compare with Fig. 7a). Then, it was possible to compare the Cu^{II} affinities of Cu^{I}–CopK and ⊠□–CopC *via* exchange reaction (29).[62]

$$\boxtimes Cu^{II}\text{–CopC} + Cu^{I}\text{–CopK} \rightleftharpoons \boxtimes\square\text{–CopC} + Cu^{I}Cu^{II}\text{–CopK} \quad (29)$$

A background correction for dimer dissociation was necessary and was estimated from Ag^{I} binding under the same conditions (Fig. 8b(ii)). The experiment demonstrated that while the affinity of *apo*-CopK for Cu^{II} is low ($K_D > 10^{-6}$ M), the affinity of Cu^{I}–CopK for Cu^{II} is much higher ($K_D \sim 10^{-13}$ M) and is similar to those of CopC and PcoC. In this example, the reference protein acted as both metal binding probe and affinity standard.

4.3.3 Affinities of HMA4n and HMA7n for Zn^{II}. HMA4 and HMA7 are two of the eight heavy-metal-transporting P_{1B}-type ATPases in the simple plant *Arabidopsis thaliana*. HMA4 transports Zn^{2+} while HMA7n transports Cu^{+}.[70,71] Their soluble N-terminal MBDs, HMA4n and HMA7n, feature a common ferredoxin βαββαβ fold (Fig. 9a) and, *in vitro*, both bind Cu^{I} and Zn^{II}.[15,58] Their affinities for Zn^{II} were estimated with the probe Mf2 (Section 3.3.7). The estimation mirrored those given in Section 4.3.1 except that the probe was based on the absorbance of the free ligand Mf2 (Fig. 2a) rather than on the fluorescence of the target protein. Titration of Mf2 (15 μM) with Zn^{2+} induced a linear decrease in absorbance at 366 nm with a turning point at $[Zn^{2+}]/[Mf2] \sim 1.0$ (Fig. 9b(i)). An equivalent titration in the presence of an equimolar concentration of HMA7n provided a steady decrease in the absorbance until $[Zn^{II}]/[Mf2] \sim 2.0$ (Fig. 9b(ii)), indicating effective competition between HMA7n

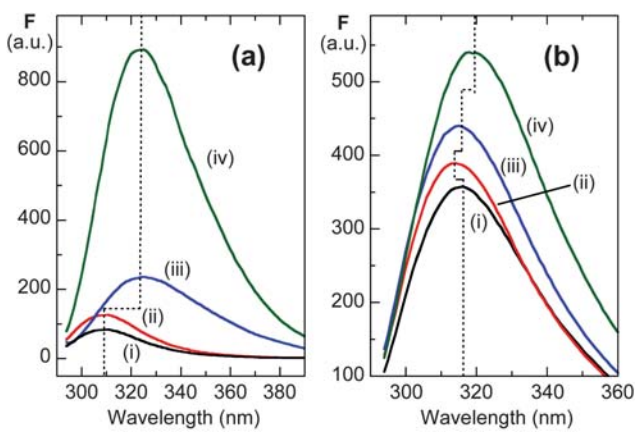

Fig. 8 (a) Fluorescence spectra for proteins (10 μM) in Mops (20 mM; pH 7.0; Na_2SO_4, 50 mM): (i) $Cu^{I}Cu^{II}$–CopK; (ii) *apo*-CopK; (iii) ⊠Cu^{II}–CopC; (iv) ⊠□–CopC. (b) Determination of $K_D(Cu^{II})$ for Cu^{I}–CopK by competition for Cu^{II} with ⊠□–CopC in the same Mops buffer: (i) initial solution containing Cu^{II} (4.5 μM), ⊠□–CopC (5.0 μM) and *apo*-CopK (20 μM) (the total intensity at 320 nm was estimated to be a 45% contribution from CopC and a 55% contribution from CopK); (ii) after addition of Ag^{+} (18 μM) into solution (i); (iii) after addition of Cu^{+} (18 μM) into solution (i); (iv) after addition of Edta (10 eq) into solution (i). Reproduced, with permission, from ref. 62.

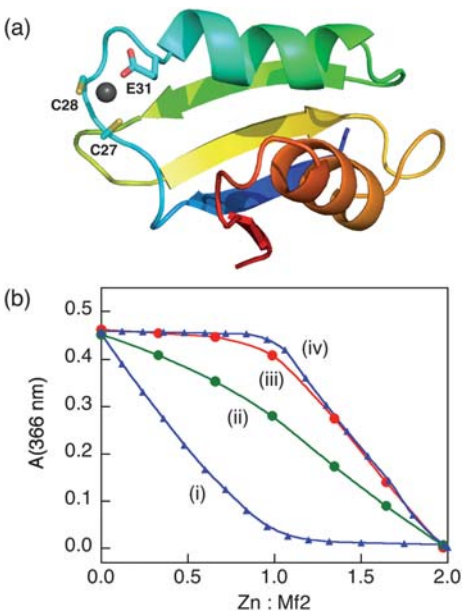

Fig. 9 (a) Ribbon representation of the Zn^{II}–HMA4n molecule (PDB code: 2KKH) highlighting Zn^{II} binding sites (Zn^{II} indicated by a gray sphere and ligands by sticks). (b) Determination of Zn^{II} dissociation constants K_D for proteins HMA2n, 4n and 7n in Mops buffer (50 mM; pH 7.3; 100 mM NaCl) with the Mf2 probe. Plots of A_{366} (proportional to free Mf2 concentration) as a function of Zn^{II}:Mf2 ratio in the presence of (i) Mf2 only; (ii) Mf2 and *apo*-HMA7n; (iii) Mf2 and *apo*-HMA4n (or *apo*-HMA2n); (iv) Mf2 and Edta. The concentration of each reagent was 15.2 μM. Reproduced, with permission, from ref. 15.

and Mf2 for the added Zn^{2+}. Quantitative analysis *via* eqns (7) and (14) estimated $K_D = 4.6(2) \times 10^{-9}$ M for Zn^{II}–HMA7n on the basis of the reported $K_D = 2.0 \times 10^{-8}$ M for Zn^{II}–Mf2,[40] *i.e.*, HMA7n has a slightly stronger affinity for Zn^{2+} than does Mf2. However, the equivalent titrations for HMA4n (~1 eq) induced little initial spectral change until the ratio $[Zn^{II}]/[Mf2] \sim 1$ (Fig. 9b(iii)), *i.e.,* until HMA4n was almost saturated with Zn^{II}. This behaviour is similar to that seen with the high-affinity Zn^{II} ligand Edta (Fig. 9b(iv)). These experiments demonstrate that the Zn^{II} affinity of HMA4n is higher than that of HMA7n and is, in fact, too high to be quantified reliably with the Mf2 probe due to its restricted Zn^{2+} buffering range (Fig. 2c). Similar examples have been reported for other Zn^{II}-binding proteins such as ZntAn and ZnuA.[72,73] A new water-soluble bis(thiosemicarbazone) ligand was synthesised recently.[44] It binds Zn^{II} with affinity slightly higher than does Mf2 and detects the binding sensitively *via* the intense absorbance of the 1:1 complex $Zn^{II}L$ (ε, 1.8×10^4 M^{-1} cm^{-1}). This allows variation of free ligand concentration to widen the Zn^{2+} buffering range, and this system can quantify the Zn^{II} affinities of both HMA7n and HMA4n.[44] In this example, a synthetic ligand acts as both probe and affinity standard.

4.3.4 Affinity of the T4 site in CueO for Cu^{II}. CueO from *E. coli* is a multicopper oxidase involved in copper tolerance under aerobic conditions.[66] It acts as a cuprous oxidase on model substrate $[Cu^{I}(Bca)_2]^{3-}$ and as a phenol oxidase on model substrate 2,6-dimethylphenol (Dmp), depending on buffer composition and the concentration of labile Cu^{2+}.[49] In Mops buffer, which has little affinity for Cu^{2+}, CueO exhibited full Dmp oxidase activity but minimal cuprous oxidase activity. The addition of the weak Cu^{II}-binding buffer BisTris (Scheme 1; Table 1) suppressed Dmp oxidase activity but promoted cuprous oxidase activity. The effects were reversed upon addition of Cu^{2+} into the BisTris buffer (Fig. 10). These correlated effects of buffer and Cu^{2+} on both activities were attributed to the presence of a labile T4 copper site near the T1 (blue) copper centre (Fig. 11). The T4 site plays essential but distinctly different roles in the two enzyme activities.[49] When CueO acts as a cuprous oxidase, the T4 site must be empty (protein designated as □–CueO) to recruit Cu^{I} from the cuprous substrate. When CueO acts as a phenol oxidase, the T4 site must be occupied by Cu^{II} (protein designated as Cu^{II}–CueO) to mediate electron flow between the buried T1 copper center and the organic substrate. The ratio of the Cu^{II}–CueO to □–CueO forms may be expressed as $(v/v_{max})/(1 - v/v_{max})$, where v is the Dmp oxidase activity which reaches a maximum value v_{max} when the T4 site is occupied fully.

In a series of BisTris·HCl solutions (50 mM; pH 7.0) containing increasing concentrations of total Cu^{II} (5–200 μM), the Dmp oxidase activity of CueO (0.1 μM) was measured and was found to increase accordingly (Fig. 10, inset). Although $K_A' = 10^{5.14} < 10^7$ M^{-1} for the Cu^{II}–BisTris complex, the high buffer ligand concentration employed (50 mM = $10^{-1.3}$ M) ensures $[L'] \approx [L]_{total}$ and $K_A'[L'] = 10^{5.14} \times 10^{-1.3} \gg 1$. Therefore, the labile $Cu^{2+}{}_{aq}$ concentrations can be calculated from eqns (9) and (10) based on the reported apparent affinity of BisTris for Cu^{II}.[39] A linear relationship was found between the labile $Cu^{2+}{}_{aq}$ concentration (expressed as $\log[Cu^{2+}]$) and the ratio of Cu^{II}–CueO to □–CueO (expressed as $\log[(v/v_{max})/(1 - v/v_{max})]$; Fig. 10, inset). The K_D value for site T4 could then be estimated from the value of $\log[Cu^{2+}]$ that corresponded to half maximal activity: K_D, 5×10^{-9} M. This value is consistent with the observation that the enzyme Cu^{II}–CueO exhibits full Dmp oxidase activity in Mops buffer without the need for added Cu^{2+}, even at the enzyme concentrations (10^{-6}–10^{-7} M) employed routinely in the assay. However, this T4 site is labile and even weak Cu^{II} binding buffers such as BisTris and KPi can strip the metal ion and deactivate the Dmp oxidase activity completely.[49]

In this example, the enzyme activity was used as a metal binding probe and the reaction buffer as the affinity standard.

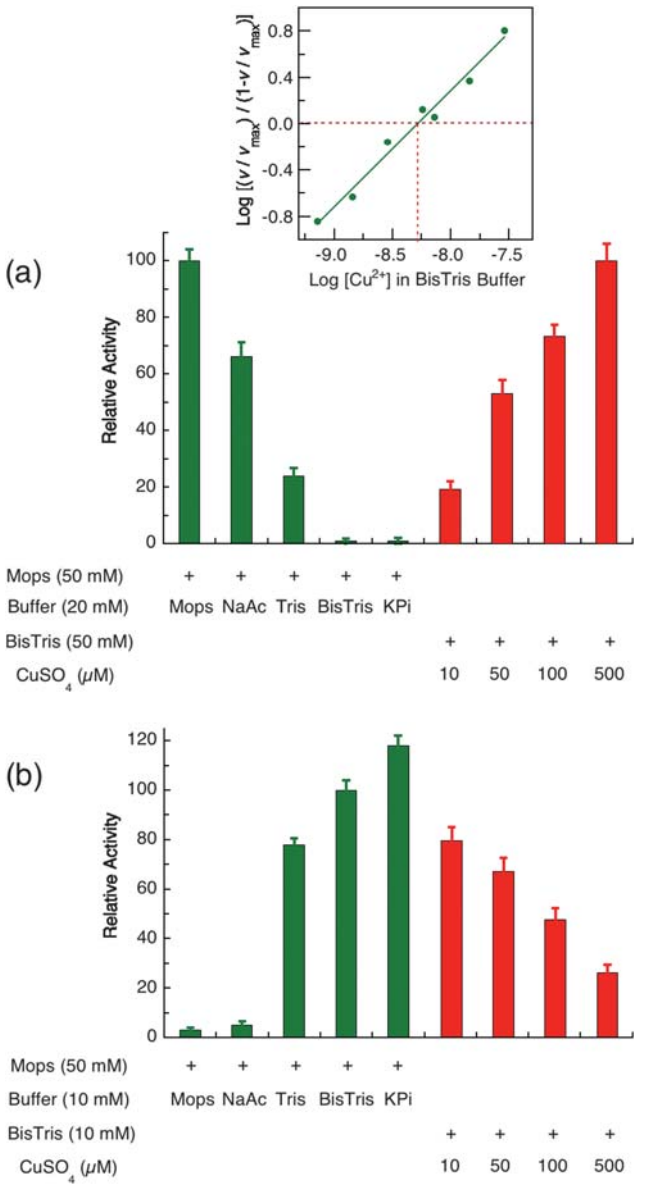

Fig. 10 Correlated effects of buffer composition (green bars) and Cu^{2+} concentration (red bars) on the oxidase activities of CueO at pH 7.0. (a) with substrate DMP (10 mM; activity normalized relative to that in Mops buffer). Inset: estimation of $K_D(Cu^{II})$ of the T4 site from the variation of DMP oxidase activity in BisTris·HCl buffer upon addition of Cu^{2+} (see text); (b) with substrate $[Cu^{I}(Bca)_2]^{3-}$ (100 μM; prepared by mixing Cu^{+} and Bca^{2+} in a 1:2.5 molar ratio; activity normalized relative to that in BisTris buffer). Reproduced with permission from ref. 49.

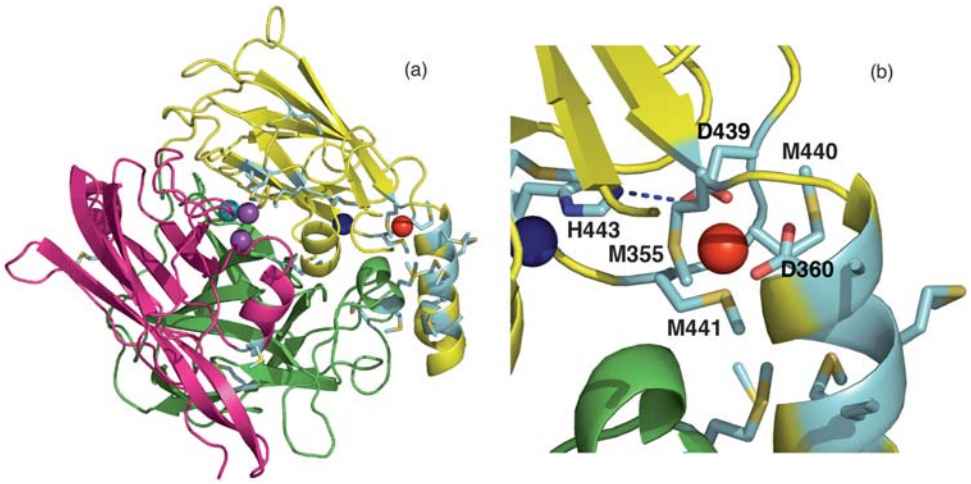

Fig. 11 Ribbon representation of the CueO molecule (PDB code: 1N68): (a) overall structure highlighting three structural domains (D1, red; D2, green; D3, gold), four defined copper centers (T1, blue; T2, teal; T3 (binuclear), purple; T4, red) and the location of methionine residues (by grey–yellow sticks); (b) molecular structure around T4 highlighting the ligands for Cu^{II}, possible ligands for Cu^{I} (including M440) and a hydrogen bond connecting the T4 copper ligand D439 and the T1 copper ligand H443.

This example also demonstrates that a pH buffer, although exhibiting weak affinity only for the metal ion (K_D, $10^{-5.14}$ M), can affect metal speciation dramatically in some cases. Consequently, careful evaluation of buffer effects is important, especially for examination of systems which bind metal ions weakly. The prion proteins and the Aβ peptides are examples (Sections 3.3.3 and 4.5).

4.4 Ligand competition involving 1:2 complexes

Eqns (8), (15) and (17) provide general formulae for competition for a metal ion M between a protein ligand P and a synthetic ligand L which forms a stable 1:2 complex ML_2. They include consideration of the affinity of L for protons. The validity of these formulae may be compromised by the presence of the 1:1 complex ML. Therefore, in addition to the challenges that were discussed for ligand probes based upon 1:1 complexes (Section 4.3), it is important to ensure that the concentration of the free ligand L in reaction (8) is sufficiently high (*i.e.*, $K_{A2}'[L'] \gg 1$) to suppress formation of the 1:1 complex. Representative examples are given in this section.

4.4.1 Affinities of PcoC, CopC, CusF and CopK for Cu^{I}. These are all periplasmic copper-binding proteins involved in copper resistance in Gram-negative bacteria.[66,68] Their Cu^{I} binding sites are rich in methionine residues but a histidine ligand may also be present in PcoC and CopC (Fig. 5a).[74] Their affinities for Cu^{I} are in the sub-picomolar range and Bca is an excellent quantitative probe for Cu^{I} binding in these proteins (see Section 3.3.9 and Fig. 4c). The data in Fig. 12 for CusF have been adapted from ref. 75 (Supplementary Figure 1) and for the other proteins from ref. 52 and 62.

Bca reacts with Cu^{I} to form a stable 1:2 complex $[Cu^{I}(Bca)_2]^{3-}$ with $\beta_2 = 10^{17.2}$ M^{-2} which is essentially pH-independent at pH ≥ 7.0 (Table 2).[41] The complex can be quantified by the absorbance at 562 nm ($\varepsilon_{562} = 7900$ M^{-1} cm^{-1}) or more sensitively at 358 nm with reference to the equivalent but copper-free Bca solution ($\varepsilon_{358} = 42\,900$ M^{-1} cm^{-1}).[52] As discussed in Section 3.3.9, in the presence of excess Bca ligand, the 1:2 complex $[Cu^{I}(Bca)_2]^{3-}$ is dominant with a negligible contribution from the 1:1 complex $[Cu^{I}(Bca)]^{-}$ (assuming that $\log K_{A1} \sim \log K_{A2}$ as suggested by ITC[12]). After addition of > 0.5 eq Cu^{+}, A_{562} does start to drop slightly and slowly over time and this may signal partial conversion of $[Cu^{I}(Bca)_2]^{3-}$ to $[Cu^{I}Bca]^{-}$ (Fig. 4b). However, such conversion would not happen under the conditions of limiting Cu^{+} concentration in the effective competition of eqn (8).

Titration of *apo*-proteins CopC, PcoC and CusF into a solution containing Cu^{I} (14.5 μM) and Bca (46 μM) induced a stepwise drop in the absorbance intensities at both 358 and 562 nm. The profiles of the spectra did not change (*e.g.*, Fig. 12b), consistent with little contribution from ternary complexes P–Cu^{I}–Bca (assuming their spectroscopic properties are different). This may be attributable to the steric hindrance provided by Bca around the Cu^{I} binding site (Scheme 1). Less than one equivalent of Cu^{I} was removed from $[Cu^{I}(Bca)_2]^{3-}$ for each equivalent of protein added, indicative of an effective competition between the protein and Bca ligands for Cu^{I} *via* eqn (8). Analysis of each set of experimental data (Fig. 12a(ii–iv)) *via* eqn (17) provided a consistent estimate of average K_D for each protein (see eqn (30) below).[52,75]

However, an equivalent titration with the CusF variant W44M led to stoichiometric removal of Cu^{I} from $[Cu^{I}(Bca)_2]^{3-}$, suggesting that the probe ligand could not compete and that this variant bound Cu^{I} with an affinity higher than that of the native protein (compare Fig. 12a(iv) and (v)).[75] The result provides a convenient and reliable definition of the 1:1 stoichiometry of high affinity binding to the variant. A simple way to confirm the high affinity is to alter the total Bca concentration under otherwise identical conditions. If eqn (8) is not competitive, the results are not sensitive to the total probe ligand concentration. A possible strategy to induce competition is to markedly increase the total Bca concentration (Fig. 4c).

The data in Fig. 12a shows that the Cu^{I} affinities increase (K_D values decrease) in the following order:

apo-CopK ($10^{-10.7}$ M) > CopC ($10^{-12.2}$) > PcoC ~ 'Cu^{II}–CopK' ($10^{-12.7}$) > CusF ($10^{-13.4}$) > W44M–CusF (<10^{-15}) (30)

The quoted K_D values are based upon $\beta_2 = 10^{17.2}$ M^{-2} for $[Cu^I(Bca)_2]^{3-}$ (Table 2; see Section 3.3.9).[41] The order in eqn (30) was confirmed by direct competition for Cu^I between *apo*-CopK and PcoC, between CopC and PcoC and between PcoC and 'Cu^{II}–CopK'. Consequently, the order is consistent with the observed properties of these proteins, which also include survival of Cu^I–CopK upon elution from a short cation-exchange column and redox shuttling of Cu^I and Cu^{II} between the individual binding sites on CopC and PcoC.[52,62,65]

An interesting aspect about the copper binding in CopK is the binding cooperativity between Cu^I and Cu^{II}. Binding of Cu^I enhances the affinity for Cu^{II} by a factor of at least 10^6 (Section 4.3.2). With the Bca probe, it was possible to demonstrate that Cu^{II} binding enhances the affinity for Cu^I. *apo*-CopK competes weakly with Bca for Cu^I, but addition of Cu^{II} also enhances the Cu^I affinity by a factor of ~10^2 (Fig. 12a(i,iii) and 12b).[62]

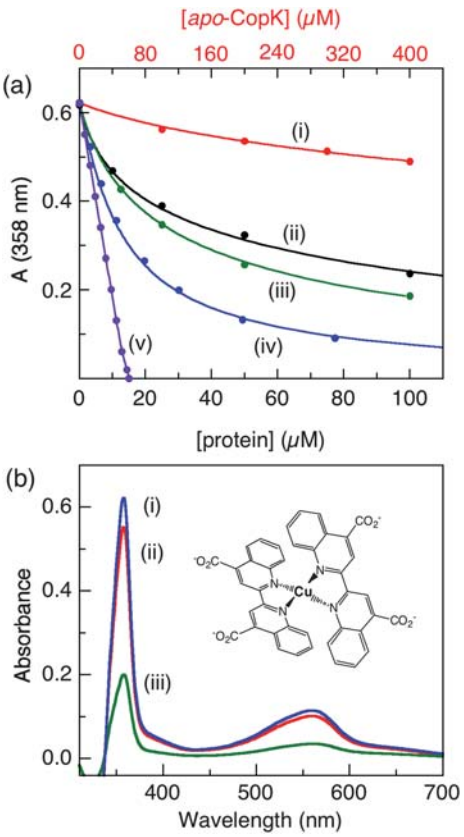

Fig. 12 Determination of Cu^I dissociation constants K_D with probe $[Cu^I(Bca)_2]^{3-}$ in Tris/Mes buffer (20 mM; pH 8.0; NaCl, 100 mM). (a) Variation of A_{358} {proportional to $[Cu^I(Bca)_2{}^{3-}]$} of a solution containing Cu^+ (14.5 μM) and Bca (~46 μM but 36 μM for CopC) with increasing concentrations of proteins: (i) *apo*-CopK (concentrations shown in red are four times that of the other proteins); (ii) *apo*-CopC; (iii) 'Cu^{II}–CopK' or *apo*-PcoC; (iv) *apo*-CusF; (v) *apo*-CusF W44M mutant. The data for CopC, CopK and PcoC were adapted from ref. 52 and 62 and the data for CusF proteins from ref. 75. For easier comparisons, A_{358} was normalised to 0.62 for a concentration of $[Cu^I(Bca)_2]^{3-}$ of 14.5 μM. The traces shown were the best fits of each of data-set to eqn (17) with average K_D given in eqn (30). The data for the W44F variant of CusF cannot be fitted. (b) Difference spectra (referenced to the same Bca solution but copper-free) of (i) a solution containing $[Cu^I(CH_3CN)_4]^+$ (14.5 μM), Bca (45 μM) and Asc (500 μM) (blue trace; substitution of Asc with Cu^{2+} (100 μM) did not change the spectrum); (ii) after addition of *apo*-CopK (100 μM) into solution (i) (red trace); (iii) as for (ii) but with Cu^{2+} (100 μM) instead of Asc (green trace). Fig. 12b was reproduced, with permission, from ref. 62.

The Cu^I affinity of CusF was re-estimated recently, again employing the Bca probe.[76] The K_D value was found to be the same, within experimental error, as that given in eqn (30) (K_D, $10^{-13.4}$ M),[75] although the new value was quoted with a lower limit of $10^{-11.3}$ M, based on $\beta_2 = 10^{14.7}$ M^{-2} rather than $10^{17.2}$ M^{-2} for $[Cu^I(Bca)_2]^{3-}$ (see Section 3.3.9). It is apparent that a reliable affinity standard is necessary in order to make meaningful quantitative comparisons. However, even when the quantitative value of the standard is in dispute, a reliable comparison can still be made by using that standard as the unit of relative affinity.[52,75] In the above examples, ligand Bca serves as both a chromophoric probe and an affinity standard.

An upper limit of $K_D = 10^{-8.1}$ M for CusF was also quoted based on $K_{A1} \sim 10^{7.4}$ M^{-1} for the $[Cu^I(Bca)]^-$ complex only.[76] But such an estimation is meaningless: (i) in the presence of excess Bca ligand, the probe A_{562} detects the 1:2 complex $[Cu^I(Bca)_2]^{3-}$ only, not the 1:1 complex $[Cu^I(Bca)]^-$ (see Fig. 4b); (ii) as discussed above and in Section 3.3.9, the relative concentration of the 1:1 complex $[Cu^I(Bca)]^-$ is negligible under the condition of $K_{A2}[L'] \gg 1$ and so only β_2 is relevant. On the other hand, for a bidentate ligand L which forms 1:1 and 1:2 complexes, even when $K_{A2}[L'] \sim 1$, *both* complexes must be considered in the K_D estimation (eqns (9) and (10)), never just the 1:1 complex.

4.4.2 Affinity of the T4 site in CueO for Cu^I. As discussed in Section 4.3.4, when CueO acts as a cuprous oxidase, the T4 site must be empty (protein designated as □–CueO) to recruit Cu^I from the cuprous substrate. This is consistent with the fact that, in the Cu^{II}-binding buffer BisTris, the enzyme exhibits maximal oxidase activity with different substrates including $[Cu^I(Bca)_2]^{3-}$ and several Cu^I-binding proteins.[49] Such a process must be driven by a high affinity of the T4 site for Cu^I (Fig. 11). However, the putative species Cu^I–CueO is a transient intermediate, and it is a difficult challenge to quantify the affinity for Cu^I *via* competition *via* eqn (8). A solution to this difficulty lies in a quantitative analysis of the steady-state kinetics of the oxidation of $[Cu^I(Bca)_2]^{3-}$ *via* an extended Michaelis–Menten equation which includes terms for the reaction rates of eqn (8) in both directions. The analysis provided a K_D value for Cu^I of ~10^{-13} M, essentially the same as that for PcoC.[49] The estimate was supported by direct competition between □–CueO and PcoC for non-redox-active Ag^I. This demonstrated that Ag^I distributed evenly between the two proteins.[49] The high affinity of the T4 site in CueO for Cu^I rationalises the observed robust cuprous oxidase activity for this enzyme with stable Cu^I substrates. PcoA, a homologue of CueO, also exhibits robust cuprous oxidase activity, likely due to the presence of an equivalent T4 site.[77] In this example, steady-state enzyme kinetics provided a concentration probe and the synthetic ligand an affinity standard.

4.4.3 Affinities of Atox1, HMA4n, HMA7n and similar proteins for Cu^I. Atox1 (also known as Hah1) is a copper chaperone in human cells which delivers Cu^I to the trans-Golgi network (TGN).[78] Atox1 features a classic ferredoxin βαββαβ fold with

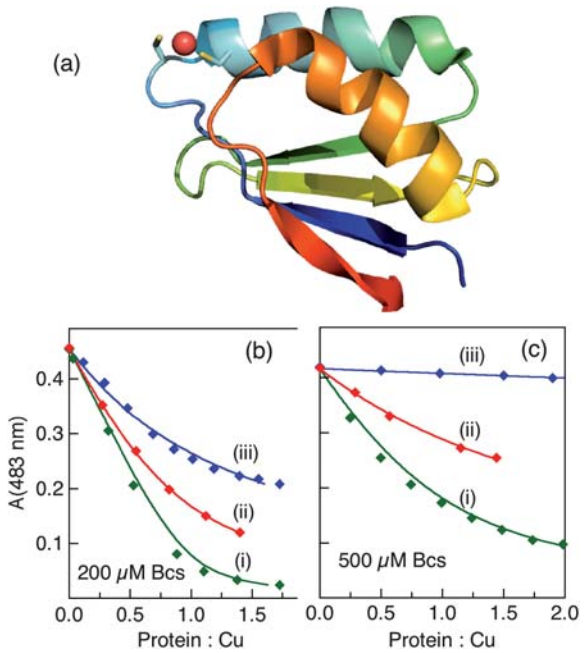

Fig. 13 (a) Ribbon representation of the Cu^{I}–Atox1 molecule (PDB code: 1FD8) highlighting the Cu^{I} binding site. (b, c) Variation of A_{483} (proportional to the concentration of $[Cu^{I}(Bcs)_2]^{3-}$) with Protein (P):Cu ratio: (i) HMA7n; (ii) Atox1; (iii) HMA4n. $[Cu^{I}]_{total}$ is within the range 32–36 μM and the position of each curve was adjusted slightly for easy comparison. In (b) $[Bcs]_{total}$ = 200 μM; in (c) $[Bcs]_{total}$ = 500 μM. The traces shown were the best fits to eqn (17) for each set of experimental data. Average K_D values are given in Table 4. Data were adapted from ref. 58 and 81.

a CxxC motif acting as a Cu^{I} binding site (Fig. 13a). Homologues of Atox1 are found in yeast (Atx1), in cyanobacteria (Atx1), in *Bacillus subtilis* (CopZ) and in many other organisms.[2,79]

As discussed in Section 4.3.3, HMA4 and HMA7 are two P_{1B}-type ATPases in the simple plant *Arabidopsis thaliana* which transport Zn^{II} and Cu^{I}, respectively. Their N-terminal MBDs HMA4n and HMA7n both feature the ferredoxin fold but have different metal binding sites (CCxxE in HMA4n *versus* CxxC in HMA7n).[15]

Each of these proteins (or protein domains) is located in the cytosol and employs cysteine instead of methionine as Cu^{I} ligands with binding affinities in the sub-femtomolar range.[11] Such high affinities fall within the Cu^{+}-buffering range of Bcs but not of Bca (Fig. 4c). Consequently, Bcs can quantify the binding affinities of these proteins and protein domains while Bca, with its lower affinity, can establish their binding stoichiometries.

The approach for Bcs *via* eqns (8) and (17) is the same as that illustrated in Fig. 12 for Bca. However, additional care must be taken when working with these cysteine-binding sites: (i) the Cys thiols are oxidized readily to the disulfide which has a very weak affinity for metal ions. So the site must be fully reduced and competition (8) should be performed under anaerobic conditions. A quantitative thiol assay (*e.g.*, Ellman[80]) is recommended to confirm both the oxidation state and the protein concentration; (ii) common reductants such as Dtt and Tcep have high affinities for Cu^{I} and must be removed completely prior to the competition. Examples of the approach are given below (see ESI‡ for details about Atox1 protein).[15,81]

After reduction with Dtt and recovery of proteins *via* a desalting column in an anaerobic glove-box, the reduced cysteine content of Atox1 (3 eq), HMA4n (2 eq) and HMA7n (2 eq) was confirmed quantitatively with Ellman reagent. Addition of each protein to a $[Cu^{I}(Bca)_2]^{3-}$ solution of composition similar to that of Fig. 12b(i) led to quantitative extraction of one equivalent of Cu^{I} from $[Cu^{I}(Bca)_2]^{3-}$. The Cu^{I} occupancy on each protein remained the same upon variation of the concentrations of *either* protein or ligand Bca, confirming high affinity binding of one equivalent of Cu^{I} for each protein (*e.g.*, Table S1‡). The protein concentrations were estimated initially *via* theoretical calculation of ε_{280} derived from the primary sequences. These were confirmed by the Ellman assay and by the stoichiometry of the high affinity Cu^{I} binding *via* $[Cu^{I}(Bca)_2]^{3-}$.[15,81] Note that the value of $\varepsilon_{280} = 2980\ M^{-1}\ cm^{-1}$ for Atox1 determined in this way is significantly smaller than that of 3884 $M^{-1}\ cm^{-1}$ estimated previously *via* amino acid hydrolysis.[10] Consistent with this difference, the previous study estimated that Atox1 bound 1.41 ± 0.22 eq Cu^{I}.

Equivalent experiments with $[Cu^{I}(Bcs)_2]^{3-}$ revealed the amount of Cu^{I} removed by each protein *via* reaction (8) to be less than one equivalent and the Cu^{I} occupancy on the protein to be sensitive to the concentrations of *both* protein and ligand Bcs (Fig. 13b,c), confirming an effective competition under certain conditions. Analysis of each set of experimental data *via* eqn (17) based on $\beta_2 = 10^{19.8}\ M^{-2}$ for $[Cu^{I}(Bcs)_2]^{3-}$ generated an average K_D value for each protein, as summarised in Table 4. Notably, although all sets of data can be fitted satisfactorily ($R > 0.98$), the two K_D values for HMA4n generated at low (200 μM) and high (500 μM) Bcs concentrations differ by one order of magnitude. HMA4n competes for Cu^{I} effectively at the low Bcs concentration but not at the high concentration (Fig. 13b(iii) *vs.* Fig. 13c(iii)) and consequently the K_D value derived from the high Bcs concentration is invalid. There is also a notable difference between the K_D values derived for HMA7n (Table 4), but in the opposite direction: HMA7n extracts Cu^{I} almost quantitatively from $[Cu^{I}(Bcs)_2]^{3-}$ at the lower Bcs concentration but competes effectively at the higher Bcs concentration (Fig. 13b(i) *vs.* Fig. 13c(i)). On the other hand, Atox1 competes for Cu^{I} effectively at both Bcs concentrations (Fig. 13b(ii) *vs.* Fig. 13c(ii)) and the two K_D values derived from these two sets of data are essentially identical, within experimental error (Table 4). These examples demonstrate that a good curve-fitting is not necessarily an indication of a reliable estimation. The best approach to ensure effective competition and reliable estimation is to perform and compare at least two sets of parallel experiments with two different ligand concentrations.

Table 4 $K_D(Cu^{I})$ (M) for proteins Atox1, HMA4n and HMA7n derived from fitting of the experimental data of Fig. 13 with eqn (17)

Protein	$[Bcs]_{total}$ = 200 μM	$[Bcs]_{total}$ = 500 μM	Adopted value
HMA4n	1.8×10^{-17}	1.2×10^{-16} [a]	1.8×10^{-17}
Atox1	4.0×10^{-18}	3.8×10^{-18}	3.9×10^{-18}
HMA7n	5.7×10^{-19} [a]	7.7×10^{-19}	7.7×10^{-19}

[a] Data unreliable due to Cu^{I} occupancies being either too high (HMA7n) or too low (HMA4n).

The data in Table 4 provide eqn (31) in order of increasing affinity (K_D decreases):

$$\text{HMA4n } (10^{-16.8}\text{ M}) > \text{Atox1 } (10^{-17.4}) > \text{HMA7n } (10^{-18.2}) \quad (31)$$

Each protein binds Cu^I with sub-femtomolar affinity, consistent with previous estimations for similar proteins or domains such as Atx1 and Ccc2n from yeast and CopZ from *Bacillus subtilis*.[11,14] These estimations are also consistent with a shallow gradient for direct Cu^I exchange between these and similar proteins.[11,12,82,83] Notably, although the zinc transporter domain HMA4n binds Cu^I with an affinity 40 times weaker than does the copper transporter domain HMA7n, it is still capable of binding Cu^I with sub-femtomolar affinity (see also Fig. 6).[15] This contrasts with a report that HMA2n (a protein domain with high sequence homology with HMA4n) bound Cu^I with an affinity of $K_D \sim 13$ μM only.[84] The latter estimation was performed by direct metal titration, which is not suitable for high affinity proteins (*cf.* Section 4.1).

Atox1 delivers copper to the TGN where the ATPase ATP7A transports it across the membrane.[78] ATP7B performs a similar role in liver cells. The genetically inherited disorders Menkes' and Wilson's diseases are associated with defects in ATP7A and ATP7B, respectively.[85] The N-termini of ATP7A and ATP7B contain six MBDs. The overall structure and metal-binding site of each domain are similar to those of Atox1.

The Cu^I binding affinities of Atox1 and MBDs of ATP7B have been determined previously with two different approaches.[10,12] The first was based on ITC experiments which estimated $K_D = 10^{-5.4}$ M for Atox1 and similar affinities for certain MBDs of ATP7B.[10] Proteins of this affinity would not compete for Cu^+ even when present at micromolar concentrations. The second estimate was based on competition for Cu^I with Bca (500 μM) and estimated K_D to be in the range 1.6–4.5 × 10^{-11} M but employed K_{A1} instead of β_2.[12] However, as discussed in Section 4.4.1, the 1:1 complex makes little contribution to metal speciation in the presence of excess Bca and a control experiment also demonstrated that the amount of Cu^I removed from $[Cu^I(Bca)_2]^{3-}$ (35 μM) by Atox1 (15 μM) was the same (~16 μM) for $[Bca]_{total} = 100$ or 500 μM (see Table S1‡),[81] *i.e.*, the affinity of Atox1 for Cu^I is too high to be buffered by Bca at 500 μM. Its behaviour is equivalent to that of the W44M variant of CusF (Fig. 12a(v)), the protein of highest affinity in eqn (30). The challenge of ensuring the effectiveness of the competition in eqns (7) and (8) is a fundamental issue in estimating metal binding affinity with this technique.

4.4.4 Affinities of HMA4n and HMA7n for Zn^{II}. These have been estimated *via* competition reaction (7) with the chromophoric probe Mf2 that binds Zn^{II} to form the 1:1 complex Zn^{II}–Mf2 with $K_D = 2.0 \times 10^{-8}$ M (Fig. 9b). While HMA7n binds Zn^{II} with an affinity falling within the Zn^{2+}-buffering range of Mf2, HMA4n binds Zn^{II} more strongly with an affinity outside that range (Section 4.3.3; *cf.* Fig. 2c). Therefore, with the Mf2 probe, only a minimum Zn^{II} affinity (*i.e.*, a maximum K_D value) can be estimated for HMA4n proteins.[15]

The ligand Par forms a 1:2 complex with Zn^{II} and has the advantage of a wider Zn^{2+}-buffering range (Fig. 2c) but the disadvantages of a marked pH sensitivity and possible

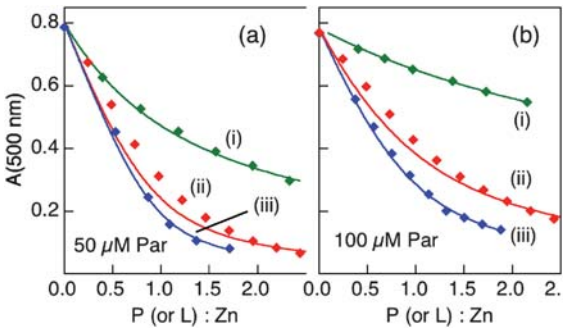

Fig. 14 Determination of Zn^{II} dissociation constants K_D for HMA4n and HMA7n proteins in Mops buffer (50 mM; pH 7.3; 100 mM NaCl) with the probe Par. Variation of A_{500} (proportional to the concentration of '$Zn^{II}(Par)_2$' with ligand:Zn ratio: (i) HMA7n; (ii) Egta; (iii) HMA4n. $[Zn^{II}]_{total} \sim 10$ μM; $[Par]_{total} = 50$ μM in (a) and 100 μM in (b). The traces shown were the best-fits to eqn (17) of each set of experimental data. Notably, the fits to the data for L = Egta were less satisfactory, suggesting possible contribution from the ternary complex. Data adapted from ref. 58.

complications with the 1:1 complex at low pH (Section 3.3.9; Table 3). The use of a non-chromophoric 'internal' standard of appropriate known affinity in the same reaction medium allows elimination of the uncertainties *via* eqns (8), (15) and (24)–(26). Egta is suitable as it competes effectively with Par for Zn^{II} at both higher (100 μM) and lower (50 μM) total Par concentrations at pH 7.3 (Fig. 14, traces (ii)). So does the protein domain HMA7n (Fig. 14, traces (i)). On the other hand, Par can compete with HMA4n at the higher concentration but is overwhelmed at the lower concentration (Fig. 14b, trace (iii) *vs.* Fig. 14a, trace (iii)). It is apparent that HMA4n binds Zn^{II} with a higher affinity than does HMA7n. The affinity of HMA7n for Zn^{II} estimated *via* this approach is the same, within experimental error, as that estimated independently *via* the probe Mf2 (Fig. 9).

4.5 Competition involving both 1:1 and 1:2 complexes

As discussed in Section 3.3.8, ligands that form both 1:1 and 1:2 complexes with relatively weak affinities under the condition of $K_{A2}'[L'] \sim 1$ must be assessed *via* both eqns (7) and (8) and be analysed with eqns (9) and (10). It is important that there are no other ligands of similar affinity be present (*e.g.*, buffer ligands). Two such examples are given in this section.

4.5.1 Affinities of Aβ peptides for Cu^{II}. The Aβ peptides of 39–43 residues are dominant constituents of the senile plaques that deposit in the brains of patients suffering Alzheimer's disease. Cu^{2+} ions appear to be linked to the neurotoxicity and self-aggregation of the peptides but their affinities for Cu^{2+} are disputed. Reported values are dispersed over five orders of magnitude in the range 10^{-6}–10^{-11} M.[45–47] The pronounced tendency for the peptides to aggregate is a serious challenge to reproducible estimation.

Gly, His and Nta (Scheme 1) were employed recently as competing ligands to estimate the binding affinities of both the monomeric and fibrillar forms (residues 1–42; 50 μM).[47] Each form displays fluorescence at 307 nm upon excitation at 280 nm, but Cu^{2+} binding quenches the fluorescence intensity linearly

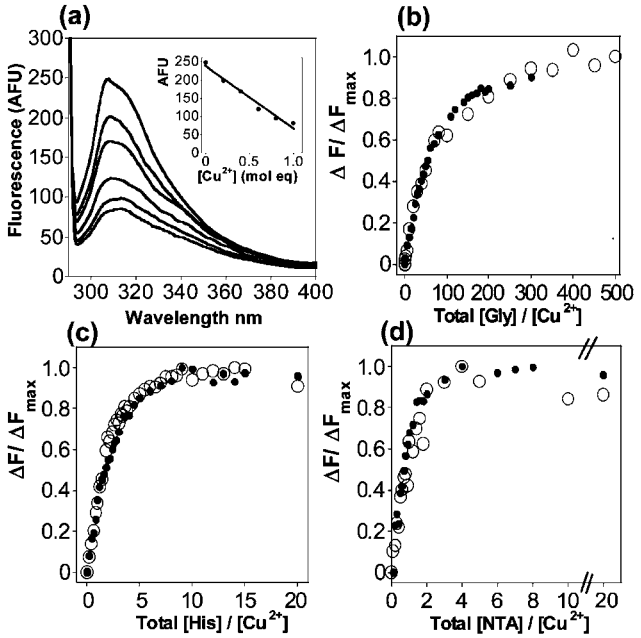

Fig. 15 Fluorescence spectra of monomeric and fibrillar Aβ(1–42) peptides. Ligands Gly, His and Nta competed with the peptides for Cu^{2+}. (a) Increasing additions of Cu^{2+} (0.2, 0.4, 0.6, 0.8, and 1.0 molar eq) to 50 μM Aβ(1–42) in water at pH 7.4 causes quenching of the tyrosine fluorescence signal. The tyrosine fluorescence signal at 307 nm returns with addition of Gly (b), His (c) or Nta (d). Monomeric Aβ(1–42) (filled circles) and fibrillar Aβ(1–42) (empty circles) in the presence of Cu^{2+} (50 μM). $\Delta F = F - F_o$ and $\Delta F_{max} = F_{max} - F_o$, where F_o is the fluorescence (307 nm) with addition of 1 eq of Cu^{2+}. Reproduced with permission from ref. 47.

until one equivalent of Cu^{II} is bound (Fig. 15a). Addition of each ligand into the system Cu^{II}–Aβ at pH 7.4 recovered the fluorescence intensity to half-maximal levels (equivalent to removal of 0.5 eq of Cu^{II} from Cu^{II}–Aβ) at different total ligand concentrations (see Fig. 15b–d and Table 5) and therefore K_D for Cu^{II} may be estimated *via* eqns (9) and (10), as outlined in the following paragraph.

It is safe to assume that the 0.5 eq of Cu^{II} removed from Cu^{II}–Aβ by ligands Gly, His and Nta exists predominantly as complexes $Cu^{II}(Gly)_2$, $Cu^{II}(His)_2$ and $Cu^{II}(Nta)$, respectively, since under such an assumption, [L′] can be calculated from eqn (10): $[Gly'] = 10^{-2.6}$ M and $[His'] = 10^{-4.5}$ M and hence $K_{A2}'[Gly'] = 10^{4.9} \times 10^{-2.6} = 200 \gg 1$ and $K_{A2}'[His'] = 10^{6.3} \times 10^{-4.5} = 63 \gg 1$. Therefore, the 1:1 complexes for L = Gly and His may be ignored under the conditions. On the other hand, Nta reacts with Cu^{II} to form a 1:1 complex only and so, from eqn (10), $[Nta'] = (0.7–0.5) \times 50 = 10$ μM. Consequently, K_D may be estimated *via* eqn (9) as given in Table 5. However, the original report[47] calculated K_D from eqn (9) using $[L]_{total}$ instead of [L′], and this results in different estimates of K_D (Table 5). The differences, although minor for L = Gly, are significant for L = His and Nta since, in the latter cases, [L′] values are much smaller than $[L]_{total}$ (see Table 5). The re-calculated K_D values are less dispersed and better match the experimental observations. For example, a re-calculated K_D value of 50 pM (but not the reported 14 pM) matches the fact that 0.7 eq of Nta can remove 50% Cu^{II} from Aβ, since Nta (K_D = 20 pM) binds Cu^{II} slightly more strongly than does Aβ. The report[47] also calculated K_D with an alternative equation (eqn (3) of ref. 47) which is, in fact, eqn (9) under the condition of $1 + K_{A1}'[L'] + K_{A1}'K_{A2}'[L']^2 \approx K_{A1}'K_{A2}'[L']^2$. However, the report again used $[L]_{total}$ instead of [L′] in the calculation.[47]

The consistency of the re-calculated K_D values (obtained with three different competing ligands) and their match with the known chemistry highlights the excellent quality of the experimental data.[47] It is also apparent that inadequate processing of experimental data can distort the estimates significantly. The average K_D value for the Aβ peptide (1–42) is about 10^{-10} M (Table 5).

4.5.2 Affinities of prion proteins for Cu^{II}. The prion protein (PrP) is a cell-surface glycoprotein with undefined physiological function. A misfolded form is believed to be responsible for the infectious prion diseases in humans, cattle and sheep.[86] Both normal and misfolded versions feature two Cu^{II}-binding regions in the unstructured N-terminal domain: the so-called octarepeat region (residues 58–91) composed of a repeating motif of eight amino acids and the amyloidogenic region (residues 90–126) between the octrepeat and the structured C-terminal domains.[7] Cu^{II}-binding has been linked to the normal function of PrP and also to the disease state.[87,88]

There is currently no consensus regarding the affinities of PrP for Cu^{II} and the reported K_D estimates are spread from 10^{-5} to 10^{-9} M with one estimate of 10^{-14} M.[5–9] Reliable estimation must overcome many difficult challenges: (i) the samples may precipitate or coagulate readily; (ii) the protein may contain multiple binding sites of differing affinities; (iii) the affinities for Cu^{II} are generally weak (weaker than those of the Aβ peptides). Even using the low affinity ligand Gly as a probe, a relatively low concentration only of Gly is necessary to ensure an effective competition. This may lead to $K_{A2}'[L'] \sim 1$ and so both 1:1 and 1:2 complexes must be considered *via* eqns (9) and (10).

Table 5 Comparison of $K_D(Cu^{II})$ for soluble and fibrillar forms of the Aβ peptide calculated *via* eqn (9)

	sol		K_D(sol)/pM		fib		K_D(fib)/pM	
Competing ligand L	$[L]_{tot}$/eq [a]	[L′]/eq [b]	Reported [c]	Re-calc. [d]	$[L]_{tot}$/eq [a]	[L′]/eq [b]	Reported [c]	Re-calc. [d]
Gly	55	54	60	62	56	55	58	60
His	1.7	0.7	6	36	1.5	0.5	8	69
Nta	0.7	0.2	14	50	0.7	0.2	14	50

[a] Equivalents of total ligand required to remove 0.5 eq of Cu^{II} from Cu^{II}–Aβ. [b] Equivalents of total ligand that does not bind Cu^{II} at half Cu^{II} occupancy on Aβ as calculated *via* eqn (10). [c] Reported K_D in as calculated *via* eqn (9) using $[L]_{total}$. [d] Re-calculated K_D *via* eqn (9) using [L′] instead of $[L]_{total}$.

Consequently, the competition systems may involve equilibria (7) and (8) at multiple sites of PrP. Such systems are sensitive to medium pH (see Section 3.3.8) and to weak affinities of the pH buffer or other potential weak ligands (see Section 4.3.4). All these complications may contribute to the dispersion of the reported affinities in the literature.[5–9] For reliable estimation and meaningful comparison, each of these potential complications must be considered and kept under control.

A few examples illustrate these challenges. Two early studies loaded PrP with multiple Cu^{2+} ions at pH 7.4 in the presence of Tris·HCl buffer (50 mM) or Gly (2 eq), but failed to take account of the competing effects of Tris or Gly and thus underestimated the affinities, reporting micromolar ranges.[89,90] Another study was performed at pH 8.0 but overlooked the effect of pH on the K_D values of Gly, leading to an overestimate of K_D, 10^{-14} M.[7] The K_D values of both PrP andGly are highly pH-dependent (eqns (21) and (23)).

Recently, Cu^{II} affinities of various PrP proteins and fragments were re-investigated by competition with Gly using visible CD as a detection probe.[9] It was apparent that, at pH 7.4, only 1–3 eq of Gly were needed to remove 0.5 eq Cu^{II}. The samples were pre-loaded with 1.0 eq of Cu^{II} (50–200 μM), suggesting weak binding. The K_D values (13–66 nM) were calculated *via* eqn (9) but used $[L]_{total}$ instead of [L′] which, although appropriate for a large excess of ligand Gly (*e.g.*, Fig. 15b), is not acceptable when the total concentration of Gly is comparable to the total concentrations of protein and Cu^{2+} (see eqn (10)). In addition, both 1:1 and 1:2 complexes must be considered in applying eqn (10) to these cases where $K_{A2}'[L'] \sim 1$ is expected (see Section 3.3.8). The actual K_D values from these experimental data are anticipated to be considerably higher than the reported values (*i.e.*, lower affinity; *cf.* Table 5).

4.6 Affinities estimated from 'free' metal concentrations buffered by synthetic ligands

In examples given above in Sections 4.3 and 4.4, the metal affinities of proteins were estimated directly from ligand competition relationships (eqn (14) or eqn (17)) where the relationships between K_D, K_A, β_2 and speciation are apparent. Equivalently, a series of 'free' metal concentrations [M] buffered by ligand L with varying metal occupancy may be calculated from eqns (9) and (10). Then, the affinity of the protein for the metal ion may be estimated by curve-fitting the variation of metal occupancy θ to eqn (5). This equivalent approach is illustrated by the following case studies.

For example, the extreme Zn^{II}-binding affinity of metal sensor/regulator protein ZntR from *E. coli* was estimated by competition for Zn^{II} with ligand *N*,*N*,*N*′,*N*′-tetrakis(2-pyridylmethyl)ethylenediamine (Tpen; Scheme 1) according to eqn (7).[91] Upon excitation at 278 nm, *apo*-ZntR yields a maximum fluorescence emission at 303 nm (characteristic of a tyrosine residue). Zn^{II} binding enhances the emission intensity by 2.6-fold, allowing the Zn^{II} occupancy of ZntR to be monitored. Tpen ($K_D = 9.3 \times 10^{-16}$ M at pH 7.0 (Table 1)[20]) can buffer free Zn^{II} concentrations between 10^{-16} and 10^{-14} M. Titration of Zn^{II} into a Tris–BisTris buffer solution (20 mM; pH 7.0) containing ZntR (10 μM) and Tpen (1.0 mM) induced a stepwise increase in the fluorescence intensity (Fig. 16a).[91] The free Zn^{II} concentration after each titration was calculated according to eqns (9) and (10), and a binding isotherm was derived as Fig. 16b. The best fit was obtained from eqn (31) (derived from and equivalent to eqn (5)) with $K_D = 10^{-14.8(3)}$ (Fig. 16b):[91]

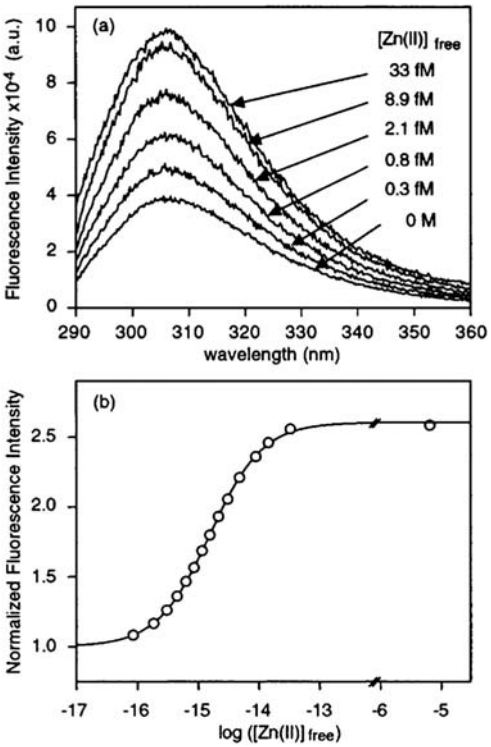

Fig. 16 Fluorescence emission spectra (a) and normalized fluorescence intensity (b) in the presence of ZntR dimer (10.0 μM) and a range of free zinc ion concentrations, monitored with excitation wavelengths of 278 nm. Conditions: 1.0 mM TPEN, 20 mM Tris–BisTris buffer (pH 7.0, *I* 0.1 M (NaCl)) at 25 °C. The solid line shows the fitted curve for eqn (32) with $\log K_D = -14.8$ ($r^2 = 0.999$). Reproduced with permission from ref. 91.

$$F = F_{min} K_D + \frac{F_{max}[Zn^{II}]_{free}}{K_D + [Zn^{II}]_{free}} \quad (32)$$

where F is the fluorescence intensity. The ZntR dimer can bind two Zn^{II} ions.[92] Eqn (32) assumes a Hill coefficient of 1.0.[91] The data indicate that ZntR binds the zinc ions non-cooperatively.[91]

In another example, the Cu^{I} affinity of porcine Cox17, a copper chaperone involved in metallation of cytochrome c oxidase, was estimated similarly according to eqn (5) with Dtt as a metal buffer and ESI-MS as a detection probe.[93] Cox17 contains six conserved cysteine residues and can bind multiple Cu^{+} ions. At neutral pH, ESI-MS detected species Cu_1–Cox17, Cu_4–Cox17 and Cu_5–Cox17 (with excess Cu^{+}) but not Cu_2–Cox17 or Cu_3–Cox17. It was suggested that, after binding of the first equivalent of Cu^{I}, Cu_1–Cox17 binds a further three equivalents cooperatively to give Cu_4–Cox17.[93] Distinctive ion-charge distribution patterns suggested that the protein undergoes conformational changes upon conversion from an open structure for the fully reduced form to a more compact structure upon Cu^{I} binding or disulfide bond formation.[93] These conclusions were consistent with those from an NMR study.[94] However, analysis of the ESI-MS data yielded a Hill coefficient of 1.35(11), consistent with a model of (essentially) non-cooperative

binding.[93] The total data were rationalized by assuming that binding of the first equivalent of Cu^{I} induced conformational changes and that this was followed by fast and cooperative binding to produce Cu_4–Cox17 and Cu_5–Cox17.[93] Unfortunately, as pointed out in Section 3.2, the question of whether gas-phase speciation reflects solution speciation has not been resolved adequately. In addition, the Cu^{I}–Dtt speciation is not well-defined due to a tendency to form multinuclear complexes.

Interesting examples of using the same approach to data processing are listed below:

(a) Cu^{I} affinity of human Sco1, a copper transporter involved in metallation of cytochrome c oxidase: estimation using NMR as the detection probe and Dtt as the metal buffer;[95]

(b) extremely high affinity of the Cu^{I} sensor CueR from *E. coli*: estimation using a CueR transcription assay as the detection probe and cyanide as the metal buffer;[96]

(c) Zn^{II} affinity of ZntA, a P_{1B}-type ATPase from *E. coli*: estimation using Mf2 as both the detection probe and the metal buffer;[73]

(d) average Cu^{I} affinity of the C-terminal domain of yeast Ctr1 (a high affinity copper importer) which binds four Cu^{I} ions cooperatively as a $Cu_4(S\text{-}Cys)_6$ cluster: estimation using Bcs as both detection probe and the metal buffer.[11]

Probes and metal buffers may vary from case to case and so may the form of data processing. However, the basic principles and challenges remains unchanged, *i.e.*, that a reliable estimation must be based on effective competition (such as eqn (7) or eqn (8)) with reliable metal affinity standards (such as those in Tables 1 and 2). If the results are in doubt, application of an independent probe or metal buffer standard is recommended.

5 Concluding remarks

Nutrient transition metals such as copper and zinc are toxic in excess or in labile 'free' forms. This dual nature constantly challenges living cells to maintain a delicate concentration balance and to ensure that the right metal is in the right place.[1,97] Cells employ multiple strategies to control metal transportation and speciation. The thermodynamic constraints are supported by evolved kinetic imperatives such as favorable molecular interactions between partner proteins. Cell compartmentalization is another strategy for overcoming large thermodynamic barriers to correct metal speciation.[3]

Accurate and reliable estimation of metal-binding affinities of partner proteins is fundamental to an understanding of these speciation strategies. At the present time, this is achieved largely by *in vitro* evaluation of isolated proteins. However, the complexity of the protein molecules presents many difficult challenges to reliable estimation of these affinities. Equilibrium competition for metal ions between the target protein ligand and a ligand of known affinity appears to be the most effective and reliable approach presently available. The competition mimics cellular conditions in terms of available metal concentration and eliminates interference from weaker or adventitious binding sites. The approach is based on the final equilibrium position only and is rarely affected by the initial metal speciation before the equilibrium reaction. Key issues in implementing this approach successfully include: (i) establishment of effective competition *via* reactions such as (7) and (8); (ii) estimation of the equilibrium concentration of at least one member of the equilibrium; (iii) estimation of the affinity of the competitor ligand; (iv) evaluation of the impact of weak binding effects from pH buffers and other potential ligands and (v) correct analysis, interpretation and processing of the experimental data.

6 Abbreviations

Aβ	amyloid-β peptides of Alzheimer's disease
Bca	bicinchoninic anion
Bcs	bathocupröine disulfonate
BisTris	2-[bis(2-hydroxyethyl)amino]-2(hydroxymethyl)-l,3-propanediol
Bq	2,2-biquinolyl
Cdta	1,2 cyclohexylene-dinitrilotetraacetic acid
Dmp	2,6-dimethylphenol
Dtt	dithiothreitrol
Edta	*N*,*N*,*N*′,*N*′-ethylenediaminetetraacetic acid
Egta	ethyleneglycol-*O*,*O*′-bis(2-aminoethyl)-*N*,*N*,*N*′,*N*′-tetraacetic acid
Gly	glycine
Hedta	*N*-(2-hydroxyethyl) ethylenediamine-*N*,*N*′,*N*′-triacetic acid
His	histidine
HMA	heavy metal ATPase
ITC	isothermal titration calorimetry
MBD	metal-binding domain
Mf2	mag-fura-2
Mops	3-(*N*-morpholino)propanesulfonic acid
Nec	neocuproine
Nta	nitrilotriacetic acid
Par	4-(2-pyridylazo)resorcinol
PrP	prion protein
Tcep	tris(2-carboxyethyl)phosphine
Tpen	*N*,*N*,*N*′,*N*′-tetrakis(2-pyridylmethyl)ethylenediamine

7 Acknowledgements

Work in the authors' laboratory was supported by research grants DP1093345 and DP0877156 from the Australian Research Council. We thank colleagues and past and present students for their insight and skilled experimentation.

8 References

1 L. A. Finney and T. V. O'Halloran, *Science (New York, N.Y.)*, 2003, **300**, 931–936.
2 S. Tottey, D. R. Harvie and N. J. Robinson, *Acc. Chem. Res.*, 2005, **38**, 775–783.
3 S. Tottey, K. J. Waldron, S. J. Firbank, B. Reale, C. Bessant, K. Sato, T. R. Cheek, J. Gray, M. J. Banfield, C. Dennison and N. J. Robinson, *Nature*, 2008, **455**, 1138–1145.
4 E. Gaggelli, H. Kozlowski, D. Valensin and G. Valensin, *Chem. Rev.*, 2006, **106**, 1995–2044.
5 R. M. Whittal, H. L. Ball, F. E. Cohen, A. L. Burlingame, S. B. Prusiner and M. A. Baldwin, *Protein Sci.*, 2000, **9**, 332–343.
6 J. H. Viles, D. Donne, G. Kroon, S. B. Prusiner, F. E. Cohen, H. J. Dyson and P. E. Wright, *Biochemistry*, 2001, **40**, 2743–2753.

7 G. S. Jackson, I. Murray, L. L. Hosszu, N. Gibbs, J. P. Waltho, A. R. Clarke and J. Collinge, *Proc. Natl. Acad. Sci. U. S. A.*, 2001, **98**, 8531–8535.
8 C. S. Burns, E. Aronoff-Spencer, G. Legname, S. B. Prusiner, W. E. Antholine, G. J. Gerfen, J. Peisach and G. L. Millhauser, *Biochemistry*, 2003, **42**, 6794–6803.
9 R. C. Nadal, P. Davies, D. R. Brown and J. H. Viles, *Biochemistry*, 2009, **48**, 8929–8931.
10 A. K. Wernimont, L. A. Yatsunyk and A. C. Rosenzweig, *J. Biol. Chem.*, 2004, **279**, 12269–12276.
11 Z. Xiao, F. Loughlin, G. N. George, G. J. Howlett and A. G. Wedd, *J. Am. Chem. Soc.*, 2004, **126**, 3081–3090.
12 L. A. Yatsunyk and A. C. Rosenzweig, *J. Biol. Chem.*, 2007, **282**, 8622–8631.
13 R. Miras, I. Morin, O. Jacquin, M. Cuillel, F. Guillain and E. Mintz, *J. Biol. Inorg. Chem.*, 2008, **13**, 195–205.
14 L. Zhou, C. Singleton and N. E. Le Brun, *Biochem. J.*, 2008, **413**, 459–465.
15 M. Zimmermann, O. Clarke, J. M. Gulbis, D. W. Keizer, R. S. Jarvis, C. S. Cobbett, M. G. Hinds, Z. Xiao and A. G. Wedd, *Biochemistry*, 2009, **48**, 11640–11654.
16 J. S. Magyar and H. A. Godwin, *Anal. Biochem.*, 2003, **320**, 39.
17 A. Krezel and W. Maret, *J. Am. Chem. Soc.*, 2007, **129**, 10911–10921.
18 D. D. Perrin and B. Dempsey, *Buffers for pH and metal ion control*, Wiley, New York, 1974.
19 J. O. Baker, *Methods Enzymol.*, 1988, **158**, 33–55.
20 A. E. Martell and R. M. Smith, *NIST Critically Selected Stability Constants of Metal Complexes Database 46, Version 8.0, U.S. Dept. of Commerce*, NIST Standard Reference Data Program, Gaithersburg, MD, 2004.
21 J. J. Spitzer and B. Poolman, *Trends Biochem. Sci.*, 2005, **30**, 536–541.
22 R. B. Thompson, *Curr. Opin. Chem. Biol.*, 2005, **9**, 526–532.
23 T. Terai and T. Nagano, *Curr. Opin. Chem. Biol.*, 2008, **12**, 515–521.
24 E. L. Que, D. W. Domaille and C. J. Chang, *Chem. Rev.*, 2008, **108**, 1517–1549.
25 E. M. Nolan and S. J. Lippard, *Acc. Chem. Res.*, 2009, **42**, 193–203.
26 R. McRae, P. Bagchi, S. Sumalekshmy and C. J. Fahrni, *Chem. Rev.*, 2009, **109**, 4780–4827.
27 A. Albert and E. P. Serjeant, *The Determination of Ionisation Constants- A Laboratory Manual*, Cambridge University Press, London, 1984.
28 C. J. Fahrni and T. V. O'Halloran, *J. Am. Chem. Soc.*, 1999, **121**, 11448–11458.
29 A. Corsini, Q. Fernando and H. Freiser, *Inorg. Chem.*, 1963, **2**, 224–226.
30 B. R. James and R. J. P. Williams, *J. Chem. Soc.*, 1961, 2007–2019.
31 C. J. Hawkins and D. D. Perrin, *J. Chem. Soc.*, 1963, 2996–3002.
32 J. Guo and D. P. Giedroc, *Biochemistry*, 1997, **36**, 730–742.
33 A. Urvoas, B. Amekraz, C. Moulin, L. Le Clainche, R. Stocklin and M. Moutiez, *Rapid Commun. Mass Spectrom.*, 2003, **17**, 1889–1896.
34 J. Pan, K. Xu, X. Yang, W. Y. Choy and L. Konermann, *Anal. Chem.*, 2009, **81**, 5008–5015.
35 A. Velazquez-Campoy, H. Ohtaka, A. Nezami, S. Muzammil and E. Freire, *Curr. Protoc. Cell Biol.*, 2004, **Chapter 17**, Unit 17 18.
36 D. E. Wilcox, *Inorg. Chim. Acta*, 2008, **361**, 857–867.
37 A. E. Martell and R. J. Motekaitis, *The Determination and Use of Stability Constants*, VCH, New York, 1988.
38 G. Schwarzenbach, *Complexometric Titrations*, Interscience Publisher, New York, 1957.
39 K. H. Scheller, T. H. J. Abel, P. E. Polanyi, P. K. Wenk, B. E. Fischer and H. Sigel, *Eur. J. Biochem.*, 1980, **107**, 455–466.
40 T. J. B. Simons, *J. Biochem. Biophys. Methods*, 1993, **27**, 25–37.
41 Z. Xiao, P. S. Donnelly, M. Zimmermann and A. G. Wedd, *Inorg. Chem.*, 2008, **47**, 4338–4347.
42 H. Irving and R. J. P. Williams, *Nature*, 1948, **162**, 746–747.
43 C. A. Blindauer, M. T. Razi, S. Parsons and P. J. Sadler, *Polyhedron*, 2006, **25**, 513–520.
44 G. Buncic, P. S. Donnelly, B. M. Paterson, J. M. White, M. Zimmermann, Z. Xiao and A. G. Wedd, *Inorg. Chem.*, 2010, **49**, 3071–3073.
45 L. Hong, W. D. Bush, L. Q. Hatcher and J. Simon, *J. Phys. Chem. B*, 2008, **112**, 604–611.
46 L. Q. Hatcher, L. Hong, W. D. Bush, T. Carducci and J. D. Simon, *J. Phys. Chem. B*, 2008, **112**, 8160–8164.
47 C. J. Sarell, C. D. Syme, S. E. Rigby and J. H. Viles, *Biochemistry*, 2009, **48**, 4388–4402.
48 W. J. Peard and R. T. Pflaum, *J. Am. Chem. Soc.*, 1958, **80**, 1593–1596.
49 K. Y. Djoko, L. X. Chong, A. G. Wedd and Z. Xiao, *J. Am. Chem. Soc.*, 2010, **135**, 2005–2015.
50 A. G. Lappin, M. P. Youngblood and D. W. Margerum, *Inorg. Chem.*, 1980, **19**, 407–413.
51 Z. Ma, D. M. Cowart, B. P. Ward, R. J. Arnold, R. D. DiMarchi, L. Zhang, G. N. George, R. A. Scott and D. P. Giedroc, *J. Am. Chem. Soc.*, 2009, **131**, 18044–18045.
52 K. Y. Djoko, Z. Xiao, D. L. Huffman and A. G. Wedd, *Inorg. Chem.*, 2007, **46**, 4560–4568.
53 M. Tanaka, S. Funahashi and K. Shirai, *Inorg. Chem.*, 1968, **7**, 573–578.
54 J. Liu, A. J. Stemmler, J. Fatima and B. Mitra, *Biochemistry*, 2005, **44**, 5159–5167.
55 A. T. Dinkova-Kostova, W. D. Holtzclaw and N. Wakabayashi, *Biochemistry*, 2005, **44**, 6889–6899.
56 M. L. VanZile, N. J. Cosper, R. A. Scott and D. P. Giedroc, *Biochemistry*, 2000, **39**, 11818–11829.
57 Z. S. Zhou, K. Peariso, J. E. Penner-Hahn and R. G. Matthews, *Biochemistry*, 1999, **38**, 15915–15926.
58 M. Zimmermann, Z. Xiao, C. S. Cobbett and A. G. Wedd, *Chem. Commun.*, 2009, 6364–6366.
59 J. B. Hunt, S. H. Neece and A. Ginsburg, *Anal. Biochem.*, 1985, **146**, 150–157.
60 M. Pollák and V. Kubán, *Collect. Czech. Chem. Commun.*, 1979, **44**, 725–741.
61 J. M. Berg and D. L. Merkle, *J. Am. Chem. Soc.*, 1989, **111**, 3759–3761.
62 L. X. Chong, M. R. Ash, M. J. Maher, M. G. Hinds, Z. Xiao and A. G. Wedd, *J. Am. Chem. Soc.*, 2009, **131**, 3549–3564.
63 F. Arnesano, L. Banci, I. Bertini, S. Mangani and A. R. Thompsett, *Proc. Natl. Acad. Sci. U. S. A.*, 2003, **100**, 3814–3819.
64 M. Koay, L. Zhang, B. Yang, M. J. Maher, Z. Xiao and A. G. Wedd, *Inorg. Chem.*, 2005, **44**, 5203–5205.
65 L. Zhang, M. Koay, M. J. Maher, Z. Xiao and A. G. Wedd, *J. Am. Chem. Soc.*, 2006, **128**, 5834–5850.
66 C. Rensing and G. Grass, *FEMS Microbiol. Rev.*, 2003, **27**, 197–213.
67 A. K. Wernimont, D. L. Huffman, L. A. Finney, B. Demeler, T. V. O'Halloran and A. C. Rosenzweig, *J. Biol. Inorg. Chem.*, 2003, **8**, 185–194.
68 S. Monchy, M. A. Benotmane, R. Wattiez, S. van Aelst, V. Auquier, B. Borremans, M. Mergeay, S. Taghavi, D. van der Lelie and T. Vallaeys, *Microbiology*, 2006, **152**, 1765–1776.
69 B. Bersch, A. Favier, P. Schanda, S. van Aelst, T. Vallaeys, J. CovËs, M. Mergeay and R. Wattiez, *J. Mol. Biol.*, 2008, **380**, 386–403.
70 S. A. Sinclair, S. M. Sherson, R. Jarvis, J. Camakaris and C. S. Cobbett, *New Phytol.*, 2007, **174**, 39–45.
71 K. E. Woeste and J. J. Kieber, *Plant Cell*, 2000, **12**, 443–455.
72 L. Yatsunyk, J. Easton, L. Kim, S. Sugarbaker, B. Bennett, R. Breece, I. Vorontsov, D. Tierney, M. Crowder and A. Rosenzweig, *J. Biol. Inorg. Chem.*, 2008, **13**, 271–288.
73 J. Liu, S. J. Dutta, A. J. Stemmler and B. Mitra, *Biochemistry*, 2006, **45**, 763–772.
74 A. V. Davis and T. V. O'Halloran, *Nat. Chem. Biol.*, 2008, **4**, 148–151.
75 Y. Xue, A. V. Davis, G. Balakrishnan, J. P. Stasser, B. M. Staehlin, P. Focia, T. G. Spiro, J. E. Penner-Hahn and T. V. O'Halloran, *Nat. Chem. Biol.*, 2008, **4**, 107–109.
76 I. R. Loftin, N. J. Blackburn and M. M. McEvoy, *J. Biol. Inorg. Chem.*, 2009, **14**, 905–912.
77 K. Y. Djoko, Z. Xiao and A. G. Wedd, *ChemBioChem*, 2008, **9**, 1579–1582.
78 B.-E. Kim, T. Nevitt and D. J. Thiele, *Nat. Chem. Biol.*, 2008, **4**, 176–185.
79 S. J. Lin, R. A. Pufahl, A. Dancis, T. V. O'Halloran and V. C. Culotta, *J. Biol. Chem.*, 1997, **272**, 9215–9220.
80 G. L. Ellman, *Arch. Biochem. Biophys.*, 1959, **82**, 70–77.
81 S. Schimo, J. Brose, Z. Xiao and A. G. Wedd, unpublished work (see ESI).
82 D. L. Huffman and T. V. O'Halloran, *J. Biol. Chem.*, 2000, **275**, 18611–18614.
83 Z. Xiao and A. G. Wedd, *Chem. Commun.*, 2002, 588–589.

84 E. Eren, M. Gonzalez-Guerrero, B. M. Kaufman and J. M. Arguello, *Biochemistry*, 2007, **46**, 7754–7764.
85 R. M. Llanos and J. F. Mercer, *DNA Cell Biol.*, 2002, **21**, 259–270.
86 S. B. Prusiner, *Proc. Natl. Acad. Sci. U. S. A.*, 1998, **95**, 13363–13383.
87 G. L. Millhauser, *Acc. Chem. Res.*, 2004, **37**, 79–85.
88 J. H. Viles, M. Klewpatinond and R. C. Nadal, *Biochem. Soc. Trans.*, 2008, **36**, 1288–1292.
89 M. P. Hornshaw, J. R. McDermott, J. M. Candy and J. H. Lakey, *Biochem. Biophys. Res. Commun.*, 1995, **214**, 993–999.
90 D. R. Brown, K. Qin, J. W. Herms, A. Madlung, J. Manson, R. Strome, P. E. Fraser, T. Kruck, A. von Bohlen, W. Schulz-Schaeffer, A. Giese, D. Westaway and H. Kretzschmar, *Nature*, 1997, **390**, 684–687.
91 Y. Hitomi, C. E. Outten and T. V. O'Halloran, *J. Am. Chem. Soc.*, 2001, **123**, 8614–8615.
92 C. E. Outten, F. W. Outten and T. V. O'Halloran, *J. Biol. Chem.*, 1999, **274**, 37517–37524.
93 P. Palumaa, L. Kangur, A. Voronova and R. Sillard, *Biochem. J.*, 2004, **382**, 307–314.
94 L. Banci, I. Bertini, S. Ciofi-Baffoni, A. Janicka, M. Martinelli, H. Kozlowski and P. Palumaa, *J. Biol. Chem.*, 2008, **283**, 7912–7920.
95 L. Banci, I. Bertini, S. Ciofi-Baffoni, I. Leontari, M. Martinelli, P. Palumaa, R. Sillard and S. Wang, *Proc. Natl. Acad. Sci. U. S. A.*, 2007, **104**, 15–20.
96 A. Changela, K. Chen, Y. Xue, J. Holschen, C. E. Outten, T. V. O'Halloran and A. Mondragon, *Science (New York, N.Y.)*, 2003, **301**, 1383–1387.
97 K. J. Waldron and N. J. Robinson, *Nat. Rev. Microbiol.*, 2009, **7**, 25–35.